

Geology of the Northern Norrbotten ore province, northern Sweden

Paper 8 (13)

Editor: Stefan Bergman



SGU

Sveriges geologiska undersökning
Geological Survey of Sweden

Geology of the Northern Norrbotten ore province, northern Sweden

Editor: Stefan Bergman

ISSN 0349-2176
ISBN 978-91-7403-393-9

Cover photos:

Upper left: View of Torneälven, looking north from Sakkaravaara, northeast of Kiruna. ***Photographer:*** Stefan Bergman.

Upper right: View (looking north-northwest) of the open pit at the Aitik Cu-Au-Ag mine, close to Gällivare. The Nautanen area is seen in the background. ***Photographer:*** Edward Lynch.

Lower left: Iron oxide-apatite mineralisation occurring close to the Malmberget Fe-mine. ***Photographer:*** Edward Lynch.

Lower right: View towards the town of Kiruna and Mt. Luossavaara, standing on the footwall of the Kiruna apatite iron ore on Mt. Kiirunavaara, looking north. ***Photographer:*** Stefan Bergman.

Head of department, Mineral Resources: Kaj Lax

Editor: Stefan Bergman

Layout: Tone Gellerstedt och Johan Sporrang, SGU

Print: Elanders Sverige AB

Geological Survey of Sweden
Box 670, 751 28 Uppsala
phone: 018-17 90 00
fax: 018-17 92 10
e-mail: sgu@sgu.se
www.sgu.se

Table of Contents

Introduktion (in Swedish)	6
Introduction	7
1. Regional geology of northern Norrbotten County	9
References	14
2. Geology, lithostratigraphy and petrogenesis of c. 2.14 Ga greenstones in the Nunasvaara and Masugnsbyn areas, northernmost Sweden	19
Abstract	19
Introduction	20
Regional setting of Norrbotten greenstone belts	21
Geology of the Nunasvaara and Masugnsbyn greenstone successions	23
Petrogenesis of the greenstones: Preliminary U-Pb geochronology, lithogeochemistry and Sm-Nd isotopic results	52
Summary and conclusions	68
Acknowledgements	69
References	70
3. Stratigraphy and ages of Palaeoproterozoic metavolcanic and metasedimentary rocks at Käymäjärvi, northern Sweden	79
Abstract	79
Introduction	80
General geology	80
Structure and stratigraphy of the Käymäjärvi area	81
Sample description	89
Analytical methods	90
Analytical results	91
Discussion	96
Conclusions	100
Acknowledgements	101
References	101
4. Petrological and structural character of c. 1.88 Ga meta-volcanosedimentary rocks hosting iron oxide-copper-gold and related mineralisation in the Nautanen–Aitik area, northern Sweden	107
Abstract	107
Introduction	108
Regional setting	108
Geology of the Nautanen–Aitik area	110
Structural geology and deformation	132
Summary and Conclusions	144
Acknowledgements	144
References	145
5. Age and lithostratigraphy of Svecofennian volcanosedimentary rocks at Masugnsbyn, northernmost Sweden – host rocks to Zn-Pb-Cu- and Cu ±Au sulphide mineralisations	151
Abstract	151
Introduction	152
Geological overview	153
Discussion and preliminary conclusions	194
Acknowledgements	197
References	198

6. Folding observed in Palaeoproterozoic supracrustal rocks in northern Sweden	205
Abstract	205
Introduction	205
Geological setting	207
Structural geological models	209
Geophysical data	212
Discussion and Conclusions	251
References	255
 7. The Pajala deformation belt in northeast Sweden:	
Structural geological mapping and 3D modelling around Pajala	259
Abstract	259
Geological setting	259
Structural analysis	263
2D regional geophysical modelling and geological interpretation	272
Local and semi-regional 3D models	274
Discussion	280
Conclusions	283
References	284
 8. The Vakko and Kovo greenstone belts north of Kiruna:	
Integrating structural geological mapping and geophysical modelling	287
Abstract	287
Introduction	287
Geological setting	289
Geophysical surveys	291
Results	296
Discussion	306
Conclusions	308
References	309
 9. Geophysical 2D and 3D modelling in the areas around	
Nunasvaara and Masugnsbyn, northern Sweden	311
Abstract	311
Nunasvaara	312
2D modelling of profile 1 and 2	316
Masugnsbyn	321
Regional modelling	329
Conclusion	338
References	339
 10. Imaging deeper crustal structures by 2D and 3D modelling of geophysical data.	
Examples from northern Norrbotten	341
Abstract	341
Introduction	341
Methodology	342
Geological setting	342
Results	345
Conclusion	358
Outlook	358
Acknowledgements	358
References	359

11. Early Svecokarelian migmatisation west of the Pajala deformation belt, northeastern Norrbotten province, northern Sweden	361
Abstract	361
Introduction	362
Geology of the Masugnsbyn area	362
Discussion	372
Conclusions	374
Acknowledgements	375
References	376
 12. Age and character of late-Svecokarelian monzonitic intrusions in northeastern Norrbotten, northern Sweden	 381
Abstract	381
Introduction	381
Geological setting	382
Analytical methods	387
Analytical results	388
Discussion	393
Conclusions	396
Acknowledgements	396
References	397
 13. Till geochemistry in northern Norrbotten	
–regional trends and local signature in the key areas	401
Abstract	401
Introduction	401
Glacial geomorphology and quaternary stratigraphy of Norrbotten	403
Samples and methods	406
Results and discussion	407
Conclusions	426
Acknowledgements	427
References	427

Introduktion

Stefan Bergman & Ildikó Antal Lundin

Den här rapporten presenterar de samlade resultaten från ett delprojekt inom det omfattande tvärvetenskapliga Barentsprojektet i norra Sverige. Projektet initierades av Sveriges geologiska undersökning (SGU) som ett första led i den svenska mineralstrategin. SGU fick ytterligare medel av Näringsdepartementet för att under en fyraårsperiod (2012–2015) samla in nya geologiska, geofysiska och geokemiska data samt för att förbättra de geologiska kunskaperna om Sveriges nordligaste län. Det statligt ägda gruvbolaget LKAB bidrog också till finansieringen. Projektets strategiska mål var att, genom att tillhandahålla uppdaterad och utförlig geovetenskaplig information, stödja prospekterings- och gruvindustrin för att förbättra Sveriges konkurrenskraft inom mineralnäringen. Ny och allmänt tillgänglig geovetenskaplig information från den aktuella regionen kan hjälpa prospekterings- och gruvföretag att minska sina risker och prospekteringskostnader och främjar därigenom ekonomisk utveckling. Dessutom bidrar utökad geologisk kunskap till en effektiv, miljövänlig och långsiktigt hållbar resursanvändning. All data som har samlats in i projektet lagras i SGUs databaser och är tillgängliga via SGU.

Syftet med det här delprojektet var att få en djupare förståelse för den stratigrafiska uppbyggnaden och utvecklingen av de mineraliserade ytbergarterna i nordligaste Sverige. Resultaten, som är en kombination av ny geologisk kunskap och stora mängder nya data, kommer att gynna prospekterings- och gruvindustrin i regionen i många år framöver.

Norra Norrbottens malmprovins står för en stor del av Sveriges järn- och kopparmalmsproduktion. Här finns fyra aktiva metallgruvor (mars 2018) och mer än 500 dokumenterade mineraliseringar. Fyndigheterna är av många olika slag, där de viktigaste typerna är stratiforma kopparmineraliseringar, järnformationer, apatitjärnmalm av Kirunatyp och epigenetiska koppar-guldmineraliseringar. En vanlig egenskap hos de flesta malmer och mineraliseringar i Norr- och Västerbotten är att de har paleoproterozoiska vulkaniska och sedimentära bergarter som värdbergart. För undersökningarna valdes ett antal nyckelområden med bästa tillgängliga blottningsgrad. De utvalda områdena representerar tillsammans en nästan komplett stratigrafi i ytbergarter inom åldersintervallet 2,5–1,8 miljarder år.

Rapporten består av tretton kapitel och inleds med en översikt över de geologiska förhållandena, som beskriver huvuddragen i de senaste resultaten. Översikten följs av fyra kapitel (2–5) som huvudsakligen handlar om litostratigrafi och åldersbestämningar av ytbergarterna. Huvudämnet för de därpå följande fem kapitlen (6–10) är 3D-geometri och strukturell utveckling. Därefter kommer två kapitel (11–12) som fokuserar på U-Pb-datering av en metamorf respektive intrusiv händelse. Rapporten avslutas med en studie av geokemin hos morän i Norra Norrbottens malmprovins (kapitel 13).

Introduction

Stefan Bergman & Ildikó Antal Lundin

This volume reports the results from a subproject within the Barents Project, a major programme in northern Sweden. The multidisciplinary Barents Project was initiated by SGU as the first step in implementing the Swedish National Mineral Strategy. SGU obtained additional funding from the Ministry of Enterprise and Innovation to gather new geological, geophysical and till geochemistry data, and generally enhance geological knowledge of northern Sweden over a four-year period (2012–2015). The state-owned iron mining company LKAB also helped to fund the project. The strategic goal of the project was to support the exploration and mining industry, so as to improve Sweden's competitiveness in the mineral industry by providing modern geoscientific information. Geological knowledge facilitates sustainable, efficient and environmentally friendly use of resources. New publicly available geoscientific information from this region will help exploration and mining companies to reduce their risks and exploration costs, thus promoting economic development. All data collected within the project are stored in databases and are available at SGU.

This subproject within the Barents Project aims to provide a deeper understanding of the stratigraphy and depositional evolution of mineralised supracrustal sequences in northernmost Sweden. The combined results in the form of new geological knowledge and plentiful new data will benefit the exploration and mining industry in the region for many years to come.

The Northern Norrbotten ore province is a major supplier of iron and copper ore in Sweden. There are four active metal mines (March 2018) and more than 500 documented mineralisations. A wide range of deposits occur, the most important types being stratiform copper deposits, iron formations, Kiruna-type apatite iron ores and epigenetic copper-gold deposits. A common feature of most deposits is that they are hosted by Palaeoproterozoic metavolcanic or metasedimentary rocks. A number of key areas were selected across parts of the supracrustal sequences with the best available exposure. The areas selected combine to represent an almost complete stratigraphic sequence.

This volume starts with a brief overview of the geological setting, outlining some of the main recent achievements. This is followed by four papers (2–5) dealing mainly with lithostratigraphy and age constraints on the supracrustal sequences. 3D geometry and structural evolution are the main topics of the next set of five papers (6–10). The following two contributions (11–12) focus on U-Pb dating of a metamorphic event and an intrusive event, respectively. The volume concludes with a study of the geochemical signature of till in the Northern Norrbotten ore province (13).

Authors, paper 8:

Stefan Luth

Geological Survey of Sweden,
Department of Mineral Resources,
Uppsala, Sweden

Johan Jönberger

Geological Survey of Sweden,
Department of Mineral Resources,
Uppsala, Sweden

Susanne Grigull

Geological Survey of Sweden,
Department of Physical Planning,
Uppsala, Sweden

8. The Vakko and Kovo greenstone belts north of Kiruna: Integrating structural geological mapping and geophysical modelling

Stefan Luth, Johan Jönberger & Susanne Grigull

ABSTRACT

A geological structural framework has been constructed for the early Palaeoproterozoic Vakko and Kovo greenstone belts, located north of Kiruna. The framework is based on a new structural geological map and a series of NW–SE-oriented profiles that show a series of N–S-striking folds and shear zones. These structures are correlated with subsurface interpretations derived from models based on gravity, magnetic and petrophysical data. The resulting model reveals a shallow to moderate south-eastward-dipping Archaean basement below metasupracrustal units. Predominantly steeply eastward-dipping shear zones bound and intersect the basement and the overlying units. A variety of shear sense indicators record formation and deformation of the belts by E–W crustal extension followed by NE–SW to E–W-directed crustal shortening, respectively. As such, the parallel-striking Vakko and Kovo belts, whose stratigraphy is almost identical, may initially have formed as separate basins or may represent a tectonic repetition. A rapid southward deepening of the Archaean basement from 2 to 3 km is apparent from the southernmost profiles. NW–SE-trending fault systems possibly accommodate part of the vertical movements causing basement deepening, but more geological and geophysical investigations are needed to confirm this hypothesis.

INTRODUCTION

Just north of Kiruna, the Vakko and Kovo belts consist of two narrow, N–S-trending greenstone belts predominantly comprising early Palaeoproterozoic sedimentary and volcanic rocks (Fig. 1). The belts are bounded by the Råstojäure Archaean basement complex to the west and north, whereas the eastern border of the Kovo belt is a contact with an oval granitic pluton intruding into the supracrustal rocks. All the rocks have been deformed and metamorphosed under low to medium-grade conditions (e.g. Bergman et al. 2001). Earlier mapping projects have assigned differing tectonic interpretations based on the observed deformational features within the belts. Vollmer et al. (1984) associated the bulk deformation with the emplacement of granitic bodies, whereas Wright (1988) and Talbot & Koyi (1995) assigned a major role to regional-scale thrusting and the formation of duplexes. More recently, Bergman et al. (2001) included the Kovo belt as a segment of the crustal-scale Kiruna–Naimakka deforma-

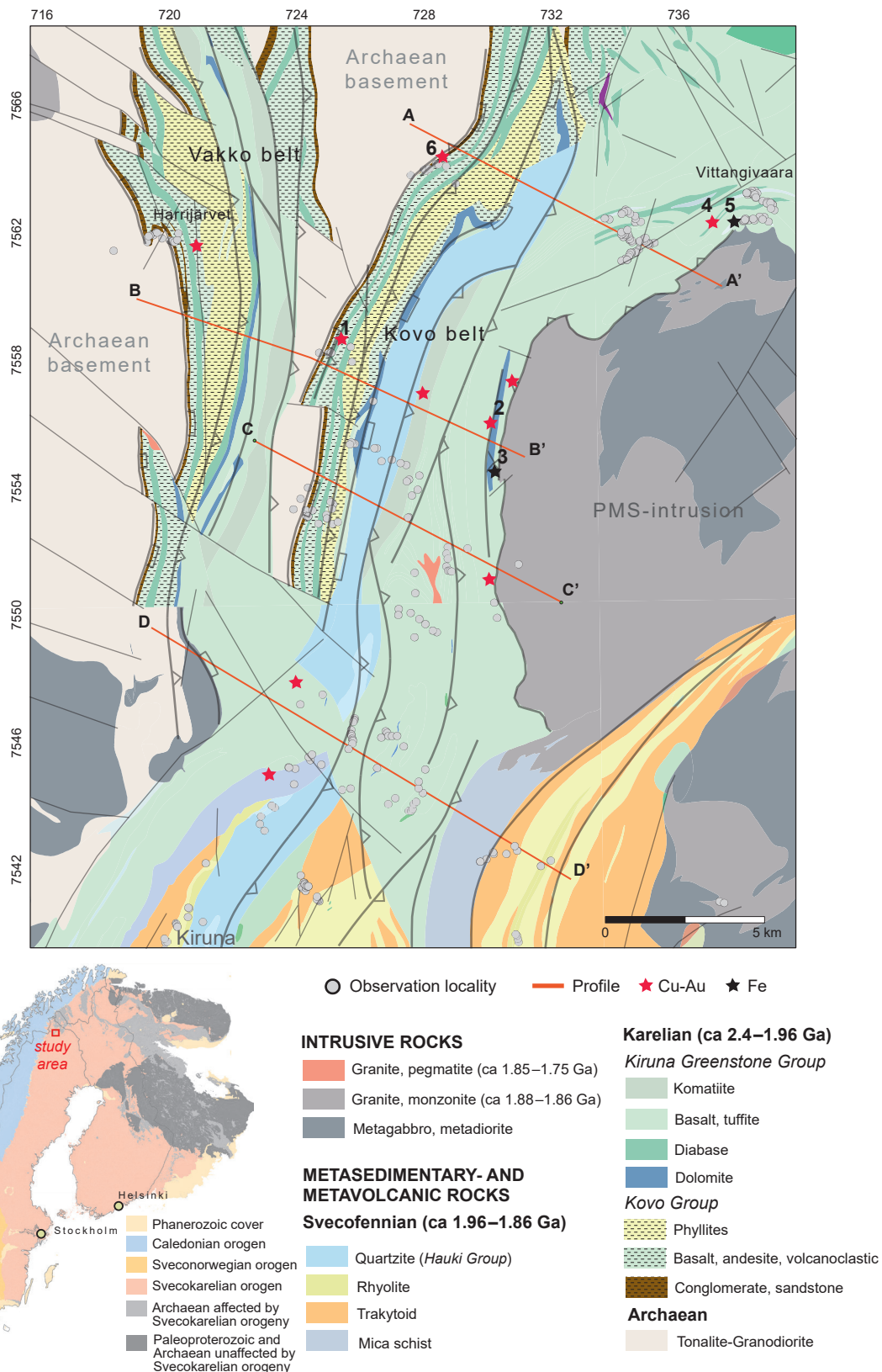


Figure 1. Geological map of the Vakkö and Kovo belts. Lithological boundaries and structural features are modified after Martinsson (1999). Indicated profiles are shown in Figure 7. Structural elements are explained in the legend for Figure 3. Numbers refer to abandoned mines, trial pits or mineralised outcrops discussed in the text: 1: Kovogruvan, 2: Linkaluoppal, 3: Tjärro, 4: Mount Vittangivaara, 5: OREDoo329, 6: Kruuvivaara. Insert map shows the main geological domains of the Fennoscandian shield.

tion zone, which accommodated dextral strike-slip movements. However, the amount of structural data obtained in these published studies is limited, rendering the above interpretations of deformation history ambiguous. On the most recent regional geological map of the area (Martinsson 1999), the extent and attitude of rock unit boundaries and shear zones were primarily derived from geophysical data, with very few constraints on deformation style and relative movements. No reliable constraints can be derived from the 3D geometry of the belt, and correlation with the Kiruna area further south is not straightforward (see Grigull et al., 2018). The latter is of major interest considering the crustal-scale structures observed in reflection seismic and audiomagnetotellurics (AMT) studies recently published by Holmgren (2013) and Bastani et al. (2015). In this study we present a new structural map of the Vakko and Kovo belts, which is the result of structural field mapping, thin-section analysis and (re)interpretation of existing and new geophysical data. Geological interpretations of 2D geophysical profiles were constructed along four lines transecting both belts and adjacent units. The results were used to interpret the 3D internal geometry of the Vakko and Kovo belts and the depth of the underlying Archaean basement. The chapter concludes with a brief discussion of regional deformation history in the context of this new information, as well as a correlation of subsurface structures with the Kiruna area.

GEOLOGICAL SETTING

The Vakko and Kovo belts comprise late Archaean to early Palaeoproterozoic metasedimentary rocks, described by Geijer (1927, 1931), Ödman (1957) and later by Martinsson (1999) and Kumpulainen (2000, 2003). A review of those earlier studies is presented in Luth & Antal Lundin (2013) and is briefly summarised below.

Archaean basement

The oldest rocks in the region form part of the Råstojåure complex, primarily consisting of 2.8 Ga-old, moderately-foliated metatonalite to metagranodiorite (Welin et al. 1971, Skiöld 1979, Martinsson et al. 1999). Biotite gneiss, reddish metagranite, metavolcanic rocks and quartzite also occur in significant quantities. However, the distribution and age of these lithologies are poorly constrained.

Kovo group

The Kovo group overlies the Archaean basement and consists of metamorphosed volcanic and sedimentary rocks subdivided into two formations. The Rautojaure formation (Martinsson 1999, Vakko unit in Kumpulainen 2000) consists of an up to 200 m thick package of metaconglomerate, containing a variety of clasts between 0.5 and 20 cm in diameter. Stream current indicators are locally well preserved in the pebble-poor interlayers of quartzite and metaarkose, indicating alluvial and fluvial deposits sourced from the Archaean terrain in the west (Kumpulainen 2000). The main part of the Kovo group consists of the 1 to 2-km-thick Harrejaure formation (Martinsson 1999), comprising volcanoclastic metasedimentary rocks interlayered with meta-tholeiitic basalt. The lavas can reach a thickness up to 200 m and often contain amygdules, commonly filled with quartz or carbonate. The interbedded layers of metavolcanic rocks consist of metavolcanic siltstones and tuffites, including sizeable feldspar and quartz grains in a matrix also containing carbonate. In the Kovo belt, the upper 300–500 m (Harrejaure formation in Martinsson 1999) consists of a phyllitic unit, characterised by well-developed schistosity. The Rautojaure and Harrejaure formations are separated by an albite-bearing metadolerite dated at 2.2 Ga (Skiöld 1986), considered to be the minimum age of the Kovo group.

Kiruna greenstone group

The Kovo group is overlain by the Kiruna greenstone group (KGG), described in detail in the Kiruna region by Martinsson (1997). The predominant rock types are mafic to ultramafic metavolcanic rocks, probably formed during a phase of intensive rifting (e.g. Kumpulainen 2000). Martinsson (1997) subdivided the Kiruna greenstone group into six formations, primarily based on differences in lithology or chemistry (Table 1). For a more detailed description the reader is referred to Martinsson (1997, 1999).

The stratigraphic sequence of the upper three formations is well exposed at Mount Vittangivaara (Fig. 1), predominantly comprising greenstone facies effusive pillow basalts, fine-grained lavas and tuffaceous rocks. Locally, the volcanic sequence alternates between metasedimentary rocks of various types, e.g. impure carbonaceous skarn to pure dolomite marble, graphite-bearing sedimentary rocks and quartz-rich schists. Quartz-banded iron-rich layers are found between pillow lava beds and between beds of massive (meta)basalt. The thin beds have an iron content of approximately 30–33 per cent and consist mainly of magnetite and hematite in equal amounts. The banded iron-rich sedimentary rocks are strongly recrystallised and alternate with thin garnet (andradite)-bearing layers.

The Kiruna greenstone group is overlain by the Kurravaara conglomerate, consisting of a basal conglomerate overlain by intermediate metavolcanic rocks. This formation is mainly exposed to the south in the Kiruna region and is described in more detail in Grigull et al. (2018).

Hauki quartzite

The youngest supracrustal unit exposed in the area is Hauki quartzite, consisting of cross-bedded feldspar metaarenite, intercalations of metasedimentary breccia and conglomerates mostly at the base of the unit. An erosional unconformity separates Hauki quartzite from the underlying Kiirunavaara group (Grigull et al., 2018). Witschard (1984) shows that the contact with the underlying rocks is often tectonic and proposes deposition of Hauki sediments in small, tectonically active grabens.

Alteration, iron, copper and gold mineralisations

Several kinds of alteration have affected the rocks of the Kovo and Vakko belts. Along shear and fault zones, extensive albite and ankerite alteration appears locally, while quartz and carbonate dykes and breccias may contain chalcopyrite. Scapolite appears as porphyroblasts in the Kiruna greenstones along the eastern border of the Kovo belt, but also occasionally in low-grade metamorphic mafic intrusions and dolerites. Epidotisation of amygdule-rich basalts is common in the Kovo belt, particularly in the lower part of the Kiruna greenstone group.

Mineralisations of copper and iron in particular have been found in the Vakko and Kovo belts (Fig. 1) but currently have no economic value. Some abandoned quarries can be found, dating back to the 16th–17th centuries, e.g. “Kovogruvan” (ORED00295), where the mineralisation consists of small concentrations of chalcopyrite, pyrite and barite in quartz veins. The veins occur in albite-bearing metadolerite and are associated with faulting in the lower part of the Kovo group. Most of the miner-

Table 1. Formations of the Kiruna greenstone group after Martinsson (1997). Youngest formation at the top.

Formation	Dominant lithology	Thickness range or maximum thickness
Linkaluoppal	Tholeiitic volcanoclastics, with layers of graphite schists, magnetite skarn, and dolomite (up to 50 m)	> 50 m
Peuravaara	Tholeiitic pillow basalts	500–1500 m
Viscaria	Basaltic tuff and thin layers of graphite schist	600 m
Pikse	Tholeiitic basalt	500–1000 m
Ädnamvare	Peridotitic and basaltic komatiite	500 m
Såkevaratjah	Dolomite (up to 200 m) and basaltic lava	200–400 m

alisations were discovered by prospecting carried out in the 1970s. The highest concentrations of copper (1.23%, Godin et al. 1979) were found at Linkaluoppal (ORED00900), and are associated with a skarn-altered metadolerite-intruding dolomitic marble, characteristic of the upper parts of the Linkaluoppal formation. The dolomitic marble has been locally altered to a skarn and contains high concentrations of barite. To the south of Linkaluoppal, iron mineralisation at Tjärro (ORED00112) was found by drilling, following geophysical measurements, and occurs as accumulations of magnetite within skarn-altered, biotite-rich tuffs of the Kiruna greenstone group. The mineralisation is the cause of a high magnetic anomaly that can be followed in magnetic survey data along a trace of approximately 9 km. The map trace of this magnetic anomaly reveals a tight syncline wrapping along the boundary, between the eastern border of the Kovo belt and the quartz-monzonite intrusion belonging to the Perthite monzonite suite (PMS) to the east.

Immediately northeast of Mount Vittangivaara a sulphide deposit was discovered based on drilling by Redmond, a prospecting company, in 1998 (ORED15581) (Fig. 1). The drill cores reveal several accumulations of pyrite, pyrrhotite and chalcopyrite associated with skarn-altered metapelites. Concentrations of copper within these 2–5-metre-intervals never exceed 2%. The iron deposit ORED00329 on Mount Vittangivaara is described by Folcker (1974) as a thin layer of altered tuff, containing the iron-rich minerals ilmenite, hematite and goethite. The graphite-bearing metapelites and schists in the area are generally fine-grained and have only a low graphite content.

Deformation and metamorphism

Earlier studies interpret the Vakko and Kovo belts as a series of synformal structures separated by shear zones (e.g. Martinsson et al. 1999). Axial planes generally trend in a north–south direction, with gently south-plunging fold axes. The area is affected by several major shear zones trending parallel to lithological contacts. The rocks in these zones display pervasive foliation and are often mylonitic. Several brittle faults have been identified, mainly interpreted from airborne magnetic data, displacing the N–S trending anomalies and appearing as linear low magnetic anomalies. Metamorphic grade varies between upper greenschist facies and lower amphibolite facies (Bergman et al. 2001). The central parts of the Kovo and Vakko belts are characterised by a relatively low metamorphic grade, which increases into the amphibolite facies along the eastern boundary of the Kovo belt with the PMS intrusions. Contact metamorphism resulted in the formation of garnet porphyroblasts within the mafic tuffs of the KGG (Martinsson et al. 1999).

GEOPHYSICAL SURVEYS

Gravity, airborne magnetic and electromagnetic (slingram) data on the Vakko and Kovo belts are presented in Figure 2. Several airborne geophysical campaigns have been carried out over the area. SGU measured the airborne total magnetic field in the early 1960s and LKAB carried out airborne measurements between 1973 and 1985, when total magnetic field, gamma radiation and electromagnetic field (both VLF and slingram) data were acquired. In addition, several ground geophysical surveys have been conducted in different parts of the area, in which magnetic or electromagnetic information has been acquired and petrophysical samples collected (Fig. 2A–B, Table 2). More information on these earlier ground geophysical surveys is presented in Luth & Antal Lundin (2013). In 2013 Bell Geospace Ltd. conducted an airborne fixed-wing campaign to collect magnetic field and gravity gradiometer FTG (Full Tensor Gradient) data over a large area of northern Sweden, including the central and northern part of the Vakko and Kovo belts. This survey was conducted at an altitude of 100–300 m, along east–west flight lines with 500 m line separation. Perpendicular tie-lines were made with a spacing of 5 km. Also in 2013 the same area was the subject of an airborne TEM (time domain electromagnetic) survey by Geotech Ltd. These measurements were made by a helicopter-based system with

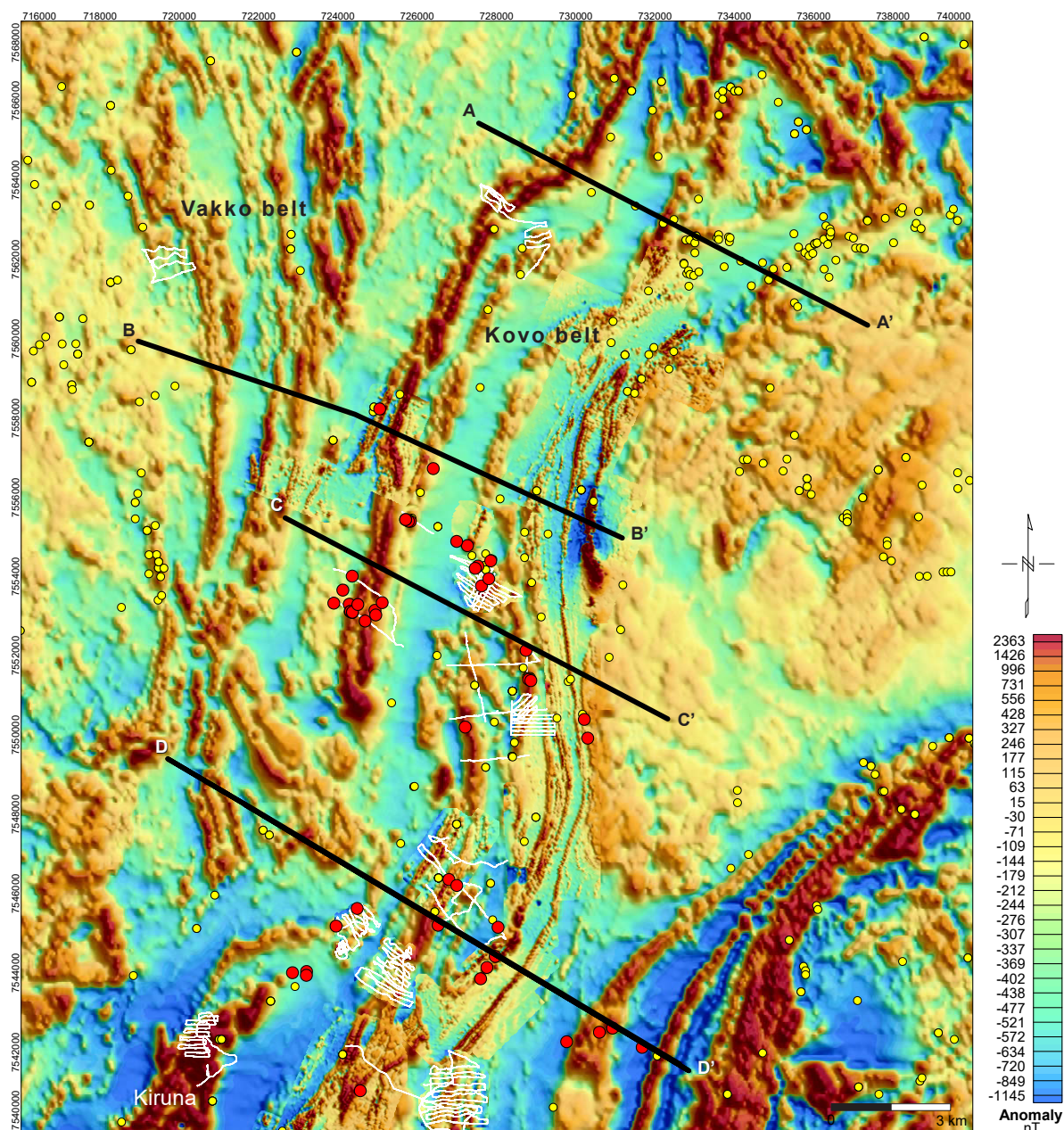


Figure 2A. Magnetic anomaly map of the Vakko and Kovo belts and adjacent areas. The magnetic data from the airborne campaigns are overlain by earlier ground magnetic surveys. Older petrophysical sample localities are displayed as yellow dots; those acquired in this project are marked with red dots. White lines represent ground magnetic profiles conducted within this project and the black lines outline the regional interpretation profiles.

the transmitter/receiver loops 56 m above the ground. The magnetic field was also measured, and the survey was carried out along east–west flight lines with 500 m line separation.

Geophysical characterisation

In the west, the Archaean basement (Råstojahre complex) is mainly composed of metamorphosed granitic to granodioritic rocks. On the magnetic anomaly map it appears as a relatively homogenous low-magnetic unit, and as a gravity low in the FTG data (Figs. 2A–B). Petrophysical samples have an average density of 2 667 kg/m³ (n=17). The contact with the adjacent Vakko belt has been investi-

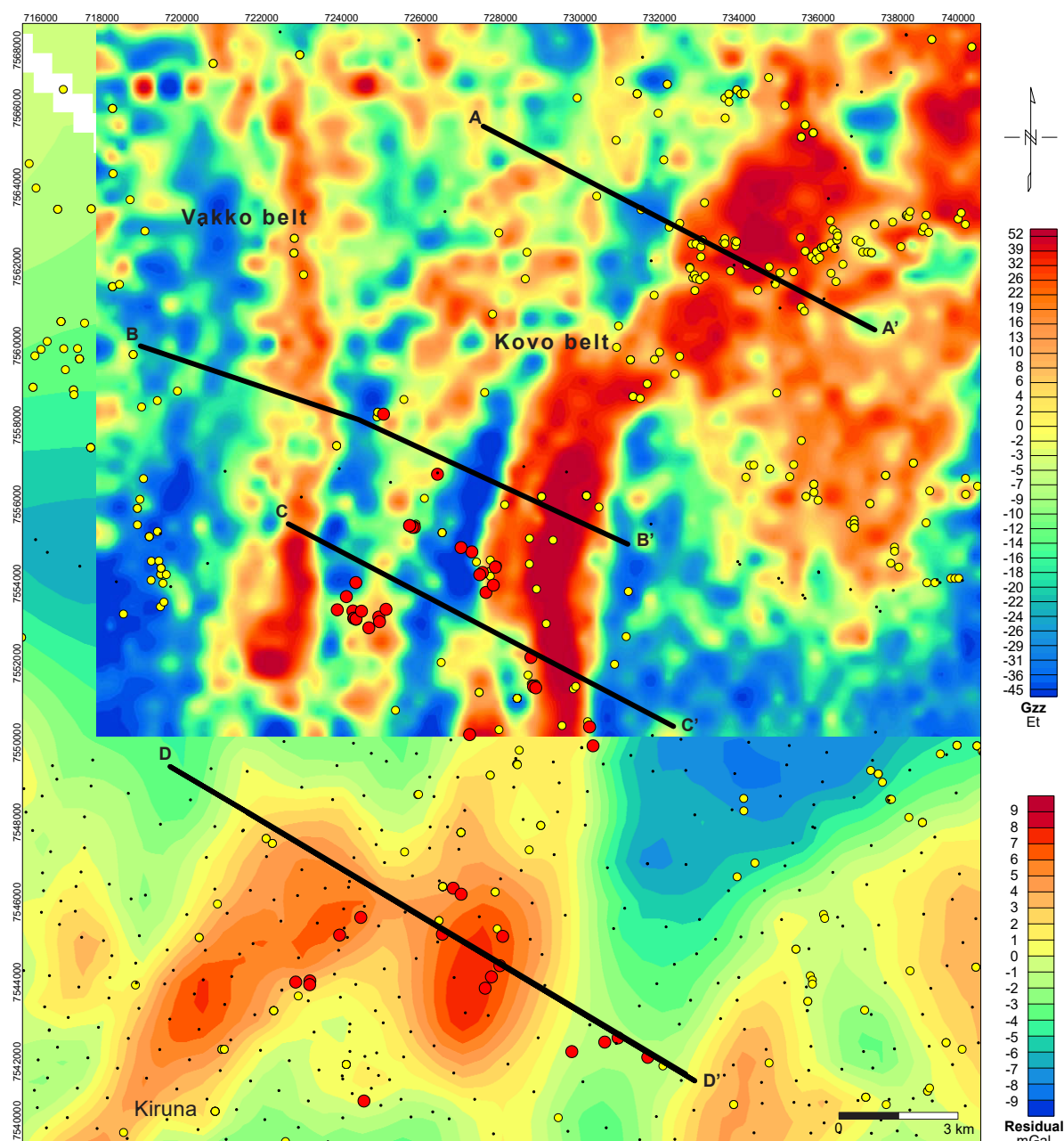


Figure 2B. Gravity anomaly map of the Vakko and Kovo belts and adjacent areas. Gravity data on the south of the area are based on ground measurements; in the north they are based on airborne FTG measurements. Black dots show the location of pre-existing ground gravity measurements. Older petrophysical sample localities are displayed as yellow dots; the red dots show the location for samples acquired in this project. The black lines outline the regional interpretation profiles.

gated by ground magnetic measurements. The Vakko belt mainly consists of metabasites, which explains the high magnetic anomalies (Fig. 2A). Petrophysical samples have densities between 2850 and 2950 kg/m³ but there is no profound positive gravity anomaly over the western part of the Vakko belt, indicating a relatively moderate depth extent of the denser rocks. However, a strong positive gravity anomaly is present over the eastern part of the Vakko belt, especially over the southernmost part, where an ultramafic volcanic rock is present. East of the Vakko belt is an Archaean basement high, which separates the Vakko belt from the Kovo belt. The Kovo belt is predominantly mafic metavolcanic rock and metadolerite, which the gravity data suggest only extends to a shallow depth. In the centre of the Kovo belt is an area of Hauki quartzite, seen on the FTG map as an elongated gravity low. Analysed

Table 2. Density and magnetic properties of the petrophysical samples from the main lithological units in the Kovozone area and its closest surroundings.

Rock type	No. of samples	Density (SI) Mean	Density (SI) Std. dev.	Susceptibility $\times 10^{-5}$ (SI) min	Susceptibility $\times 10^{-5}$ (SI) max	Susceptibility $\times 10^{-5}$ (SI) median	Q-value min	Q-value max	Q-value median
Rhyolite	10	2 643	32	18	1173	271	0.14	23.76	0.36
Dacite-rhyolite	3	2 719	17	3 570	9 011	5 580	0.07	3.50	0.35
Basalt-andesite	195	2 951	101	4	173 300	109	0.02	81.46	0.37
Mafic rock	7	2 896	47	22	5 358	99	0.04	2.37	0.38
Granite	32	2 618	22	5	4 284	664	0.08	4.71	0.31
Tonalite-granodiorite	35	2 712	36	0	14 230	74	0.05	3.12	0.28
Syenite	10	2 639	45	23	15 851	2 500	0.10	1.77	0.25
Gabbro-diorite	39	2 906	48	70	18 560	5 138	0.14	5.48	0.90
Dolerite	34	2 958	123	61	32 060	6 111	0.08	82.45	0.45
Conglomerate	7	2 693	117	3	80	51	0.29	22.07	2.07
Quartzite	20	2 644	48	1	94	6	0.29	11.99	1.12
Phyllite	9	2 724	66	12	5 444	20	0.32	9.32	1.83
Schist	5	2 730	51	14	2 001	49	0.17	1.27	0.86

petrophysical samples ($n = 20$) show the quartzite has a relatively low density, averaging $2\,644\text{ kg/m}^3$. The quartzite has a low content of magnetic minerals, reflected in a median susceptibility value of 6×10^{-5} SI units. As such, the quartzite can be followed on the magnetic anomaly map as a magnetic low. East of the quartzite, the mafic metavolcanic rocks of the KGG stand out on the gravity map as a positive anomaly, indicating, in combination with constraints derived from petrophysical measurements, that the unit has a substantial depth extent, in contrast to the “shallower” western part of the zone (see also the section *Construction of geophysical profiles*). A series of high and low magnetic anomalies within the KKG reveals a tight, N–S-striking folding pattern in the easternmost part of the Kovo belt. Strong variations in magnetic properties within the KKG are also evident in the analysed petrophysical samples (Fig. 2C, Table 2). Further north, in the Mount Vittangivaara area, a significant positive gravity anomaly correlates well with a low magnetic anomaly. Ten petrophysical samples from outcrops within this anomaly have an average density and susceptibility of $2\,980\text{ kg/m}^3$ and 80×10^{-5} SI units, respectively. The lithologies dominating this area are mafic metavolcanic rocks and metadolerite. Furthest to the east, the PMS intrusion adjacent to the Kovo belt has a low density, with an average of $2\,613\text{ kg/m}^3$ ($n = 14$). But the presence of metagabbro in the northern part of the intrusion gives rise to a positive gravity anomaly and a slightly higher magnetic anomaly.

Construction of geophysical profiles

The geophysical survey conducted for this study has focused on better constraining the structural and lithological relationships at a number of key locations (Fig. 2A). The resulting datasets include ground-based total field magnetic and electromagnetic profiles, along with measurements of the physical properties of most lithologies. These datasets, together with the airborne magnetic, FTG data or ground gravity data were then used to construct 2D geophysical subsurface models along 4 NW–SE-striking profiles. The profiles are the result of 2D modelling of geophysical potential field data (airborne or ground magnetic and gravity data). The three most northerly profiles shown in Figures 2A–C are located in an area that was part of a FTG survey conducted by Bell Geospace in 2013. The FTG survey was carried out at an altitude of 100–300 m, along east–west flight lines with an internal spacing of 500 m. Although magnetic field was also measured, the data used in the models originate from the SGU airborne survey, since that was conducted at an altitude of 30 m, the lower altitude giving considerably more information. “Potent” modelling software was used to construct these models. Background properties in the models were set at $2\,700\text{ kg/m}^3$ for density and 100×10^{-5} SI units for magnetic

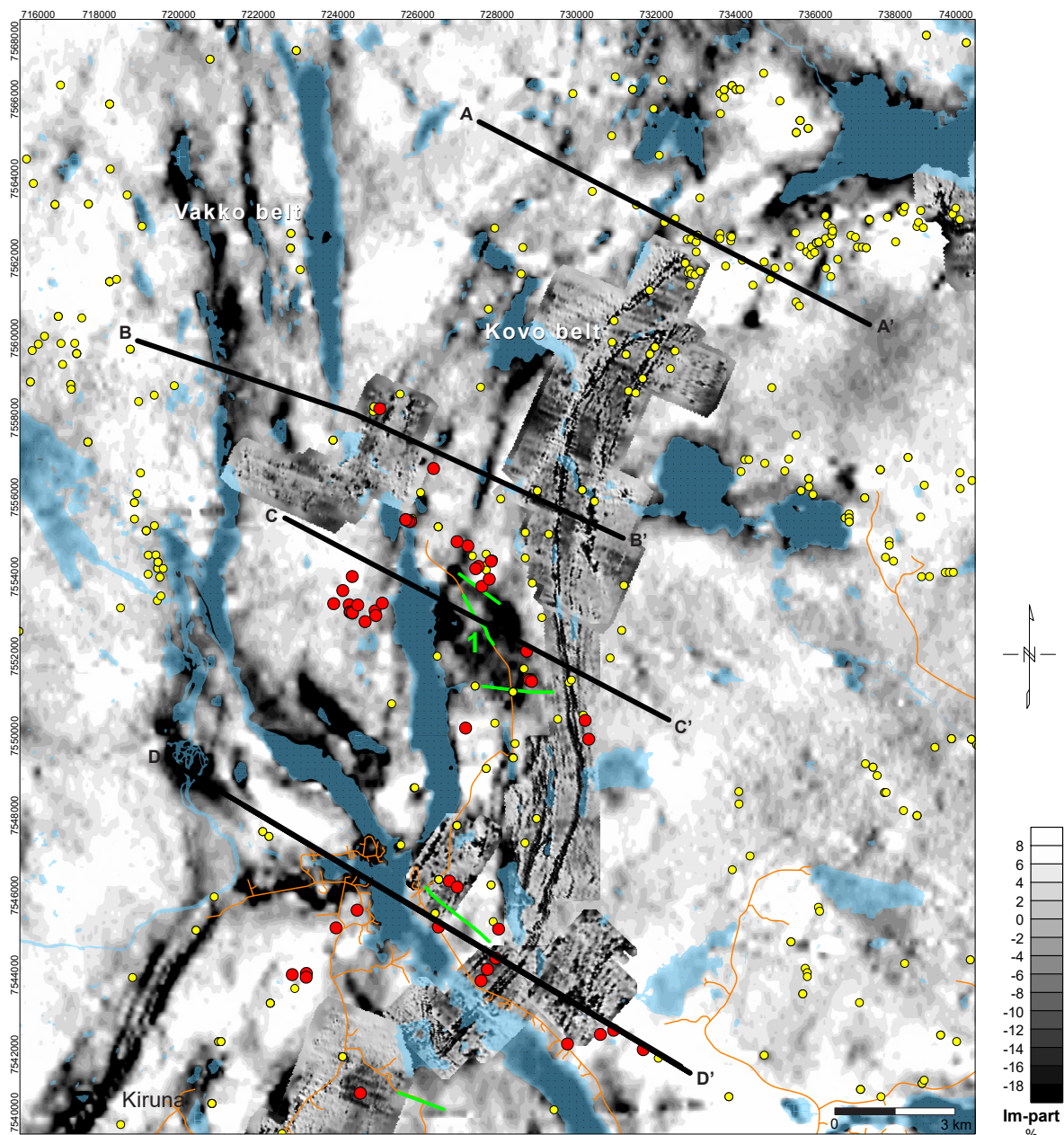


Figure 2C. Airborne slingram map of the Kovo and Vakko belts and adjacent areas. Older petrophysical sample localities are displayed as yellow dots; the red dots show the location for samples acquired in this project. Green lines show the location of ground profiles using a VLF instrument under this project, and the black lines outline the modelled profiles.

susceptibility. The magnetic and gravity data were used to constrain the depth extent of the various lithologies traversed by the profiles. The results from ground measurements using a magnetometer or VLF instrument carried out for this study were adopted in the modelling work. Densities and magnetic properties obtained from petrophysical samples and in situ measurements of magnetic susceptibilities on outcrops provided additional constraints on the modelled geometries (Fig. 2D).

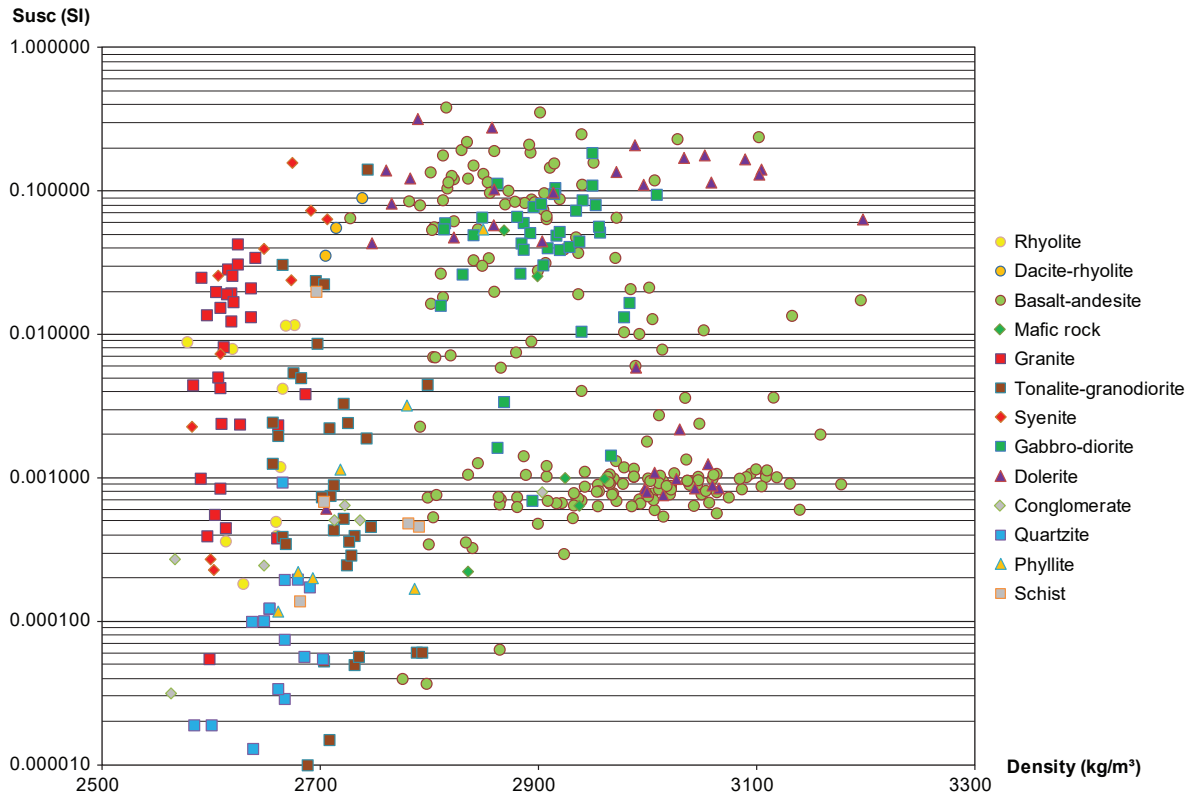


Figure 2D. Magnetic susceptibility vs. density of the petrophysical samples from the main lithological units in the Kovo belt and its immediate surroundings.

RESULTS

New structural geology map

The large-scale structural pattern of the Vakko and Kovo belts is highlighted in the new structural geology map (Fig. 3). Form lines were primarily derived from the airborne magnetic and electromagnetic anomaly maps and represent continuous lithological horizons or deformational features. Traces of the major shear zones were mainly derived from interpretations of the geophysical anomaly maps, but direct geological evidence has now been provided for most zones and is elaborated on in the following section. Kinematic symbols are based on geological observations, with the exception of some strike-slip indicators, which are only apparent from the magnetic anomaly patterns. The map trace and types of folds displayed on the structural map were constructed using a combination of geophysical and geological data, respectively. The constructed profiles provide further constraints on the mapped features in terms of dip direction and sometimes, kinematics. The new structural geological map is therefore a result of combining interpretations of surface and subsurface data.

Main deformation features

The Vakko and Kovo belts are both characterised by series of narrowly-spaced, N–S-striking folds and shear zones (Fig. 3). Many of the observed shear zones are several metres wide, strongly sheared contact zones between lithological units (e.g. Hauki quartzite). It appears from field observations that most shear zones dip steeply to moderately east, and have accommodated mainly dip-slip reverse movements in combination with a minor component of dextral strike-slip. Normal shearing has been recorded along locally folded tectonic contacts between the Kovo group and the Archaean basement, and also

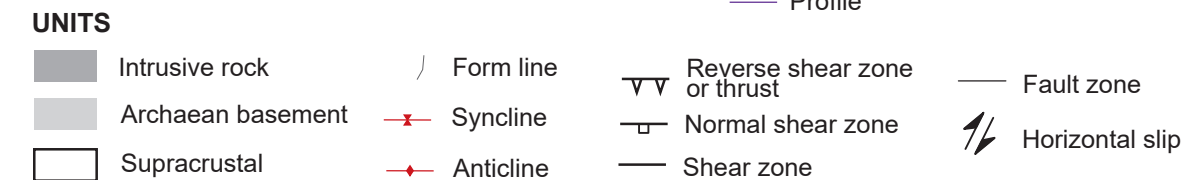
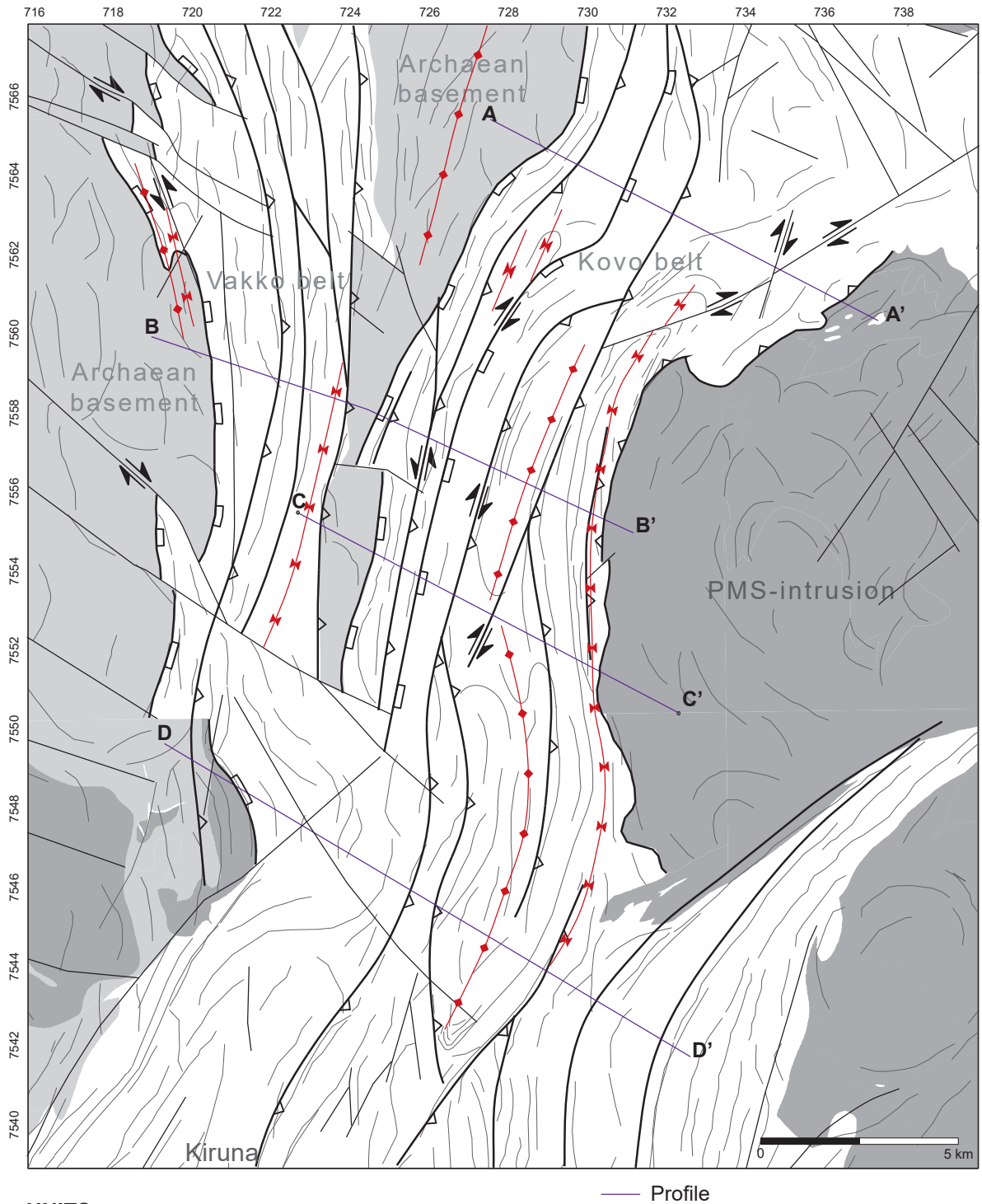


Figure 3. Compiled structural map of the Vakko and Kovo belts. The form lines were primarily derived from magnetic and slingram anomaly maps (Fig. 2a, c) and may represent continuous lithological horizons or deformational features such as tectonic foliation. Shear zones and associated kinematics are based on new field observations and Martinsson (1999), and also on geophysical anomaly maps and subsurface models presented in this study (see text for more detail). Profiles indicated are displayed in Figure 7.

along the western border between the Kovo group and the Hauki quartzite. In contrast, the eastern borders of both the Vakko and Kovo belts are marked by major reverse shear zones and by upright isoclinal folds striking parallel to the shear zones. Within the surrounding units, the observed deformation due to folding and shearing is less pronounced than within the belts. In the interior of the PMS intrusion, deformation is weak and the concentric pattern outlined by form lines may relate to a magmatic zonation (Fig. 3). The Archaean basement is locally folded and clearly fragmented along NW–SE-striking dextral faults or shear zones interpreted from the magnetic anomaly map (Fig. 3). However, deformation in the internal part of the Archaean basement has been mainly inferred from form lines striking in a N–S direction, parallel to the contact with the Vakko and Kovo belts. No deformational features related to these form lines within the Archaean basement were analysed in this study.

Structural field data

Structural data from the Vakko and Kovo belts, collected during geological field studies, are presented in stereographic plots (Fig. 4). Plotted poles to bedding planes show clusters of steeply N–NE–S–SW-striking bedding, along with shallower (20–30 °) southward-dipping bedding. The clusters can be interpreted as reflecting N–NE–S–SW folding. The plotted poles to foliation planes show a gradual variation between sub-vertical NE–SW and NW–SE-striking planes parallel to the outline of the Vakko and Kovo belts. Based on a comparison between the bedding and foliation plots, it may be stated that the foliation represents an unfolded axial plane cleavage around which the bedding is folded. Only a single phase of folding is therefore recognised. Measured fold axes also show a NE–SW trend, and vary from moderately northward to moderately southward-plunging. It should be noted that in previous studies only southward-plunging fold axes were documented. But measured intersection lineations, which are mostly oriented parallel to the fold axis, do usually plunge to the south. Stretching lineations, rarely documented in earlier studies, appear mainly to plunge steeply to the southeast, or moderately towards the southwest. Associated kinematic indicators are most consistent with an east-side-up sense of shear, but an additional component of dextral strike-slip has been derived from several horizontal outcrops and from thin sections. The type of stretching lineation depends very much on the lithology. Pencil and cigar-type lineations are often well developed in dolomitic marbles (Fig. 5C) and metaconglomerates, whereas mineral lineations defined by calcite or chlorite are more abundant in phyllitic, metavolcaniclastic siltstones (Fig. 6A–D). However, the competent basaltic units contain very few deformational features. A moderate degree of deformation is locally indicated by possibly flattened, ellipsoidal pillow metabasalts (Fig. 5D), while thin sections reveal local development of a spaced cleavage (Fig. 6E, G, H). In the eastern part of the Kovo belt along the contact with the PMS intrusion in particular, the cleavage is oriented parallel to the main foliation and is defined by mica overgrowing a partly recrystallised fabric composed of quartz and feldspar (Fig. 6E–F). Drag folds with an overall S asymmetry, indicating an eastern-side-up sense of shear. Tectonic vergence towards the west is typical of those outcrops located along or within shear zones (Figs. 5B, 6G). In contrast, away from the shear zones, mesoscopic open, upright folds were observed within the Hauki quartzite (Fig. 5E). A number of small-scale, moderately-dipping thrusts overprint the main foliation (Fig. 5F). Based on retrograde assemblages (chlorite, mica, quartz) as well as brittle-ductile microstructures, we interpret these thrusts to be relatively young features.

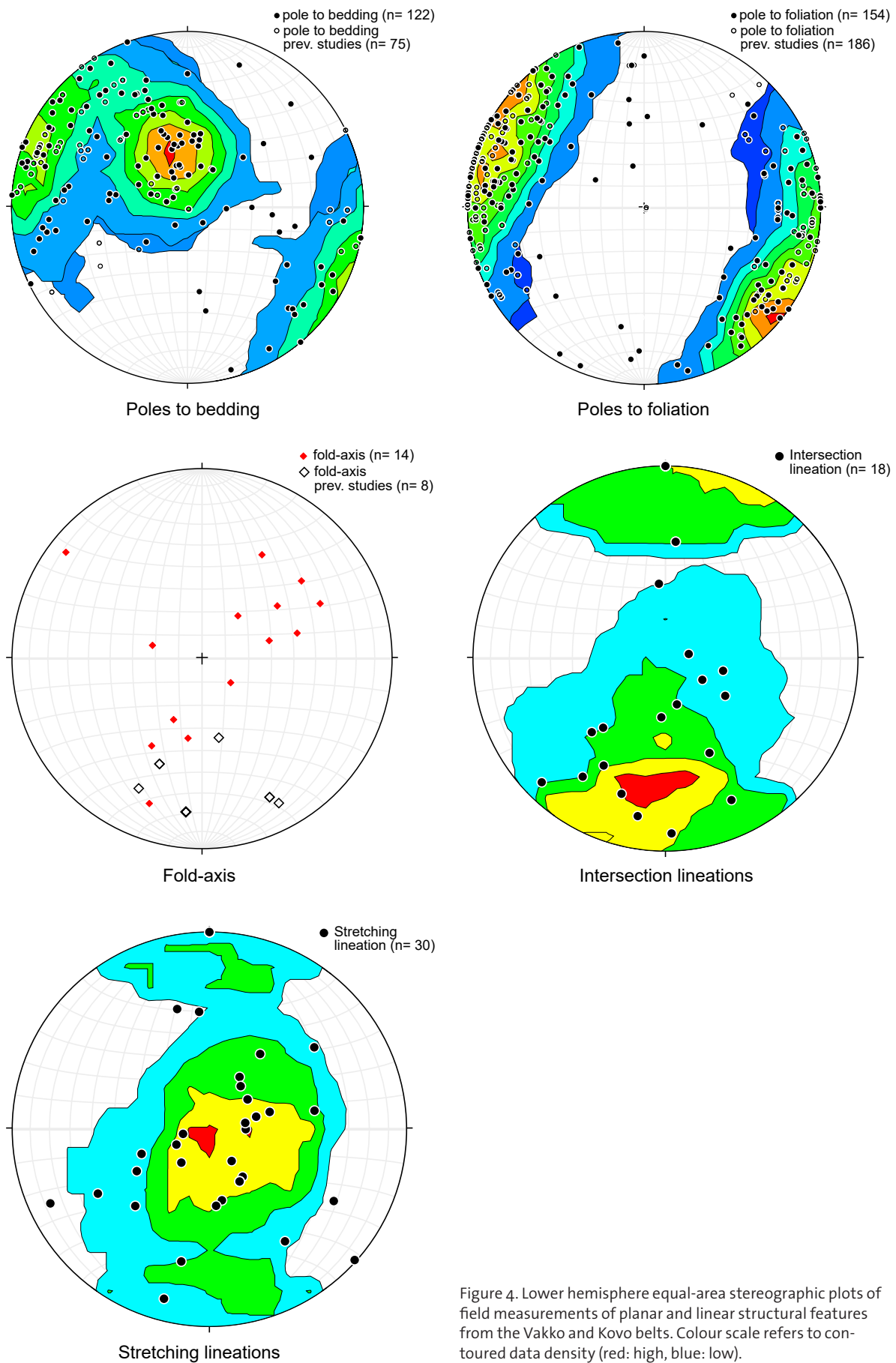


Figure 4. Lower hemisphere equal-area stereographic plots of field measurements of planar and linear structural features from the Vakko and Kovo belts. Colour scale refers to contoured data density (red: high, blue: low).

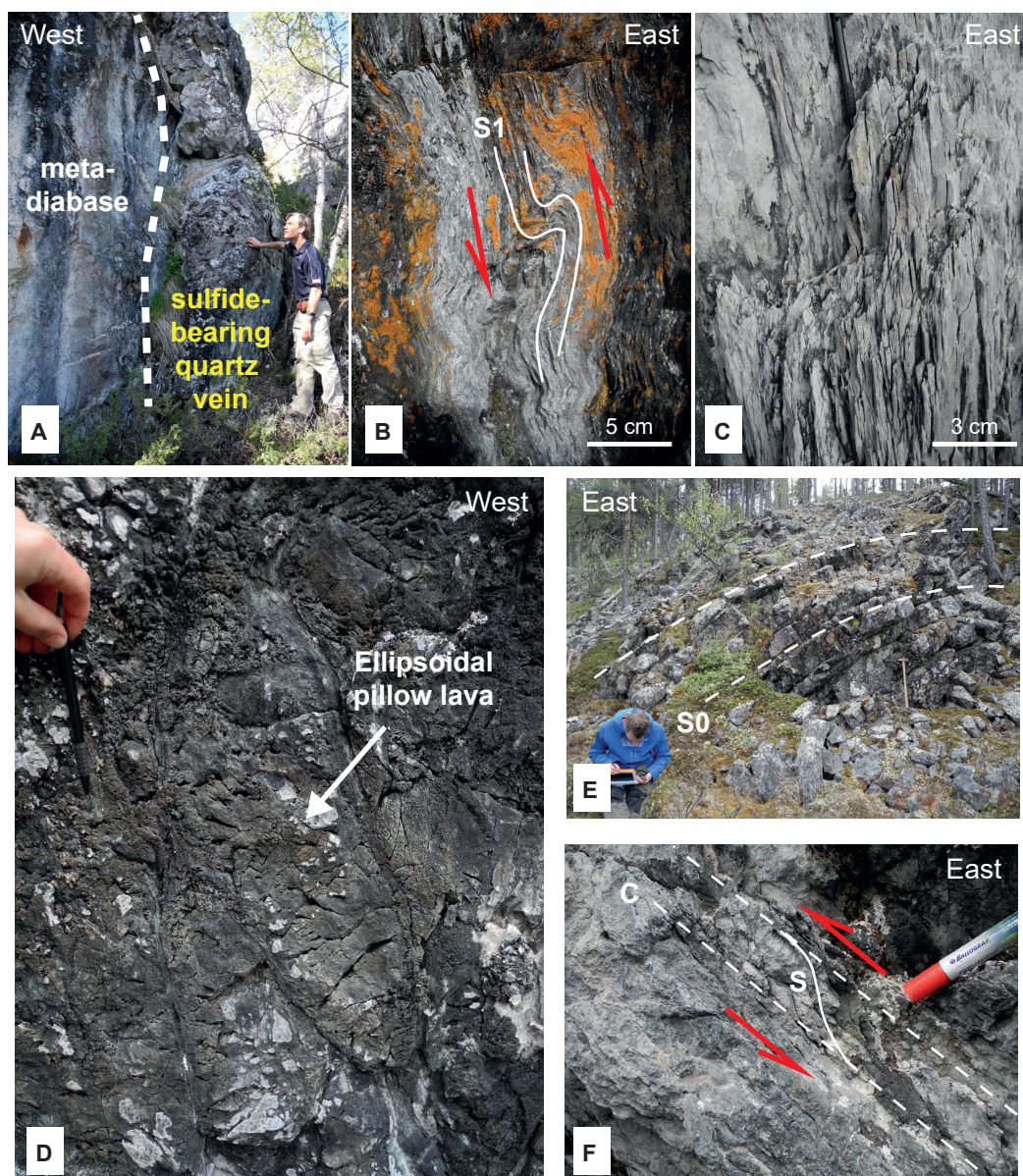
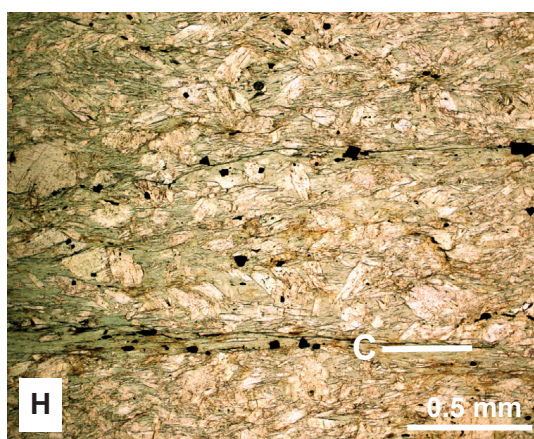
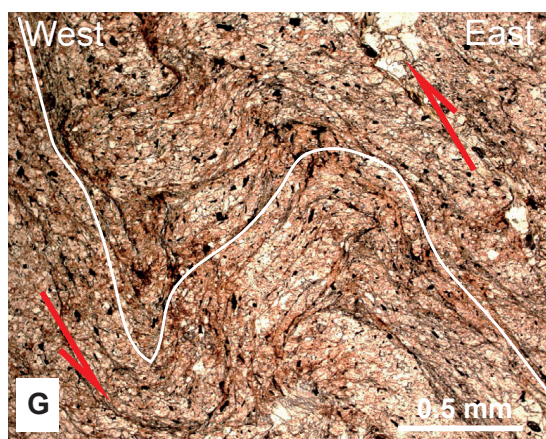
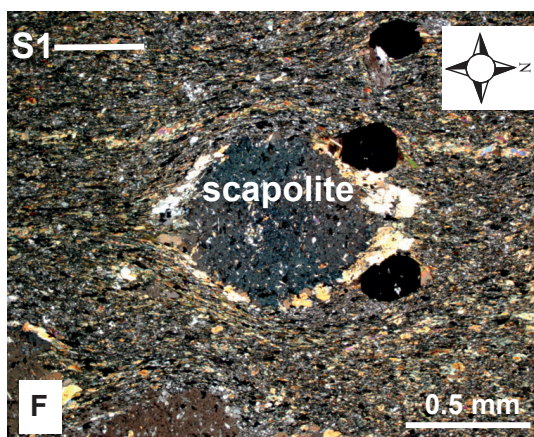
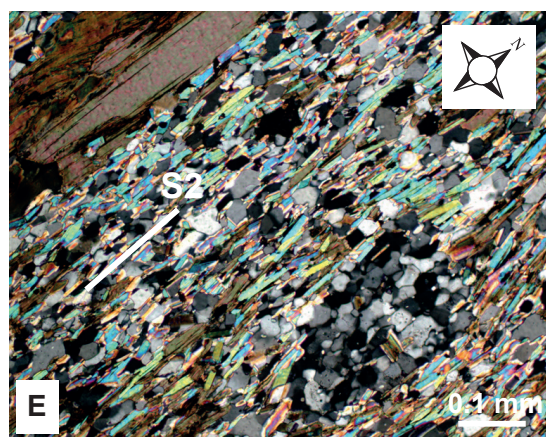
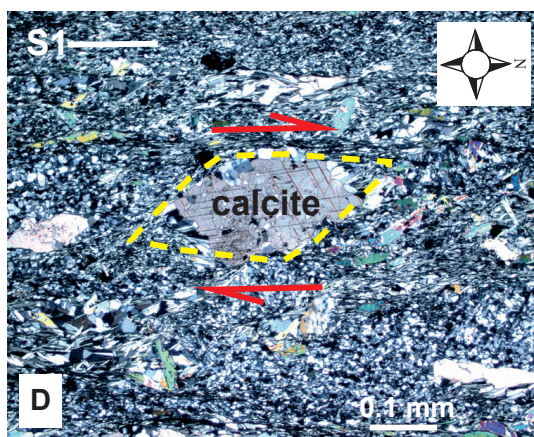
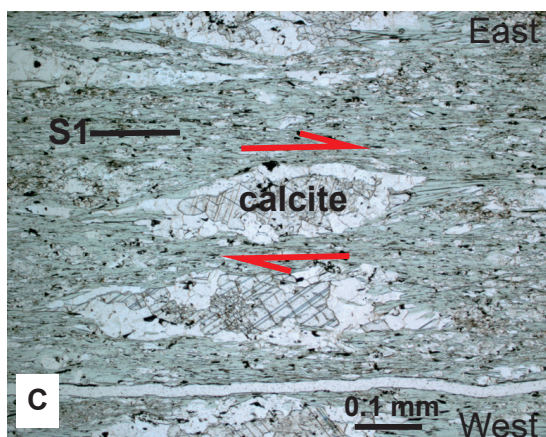
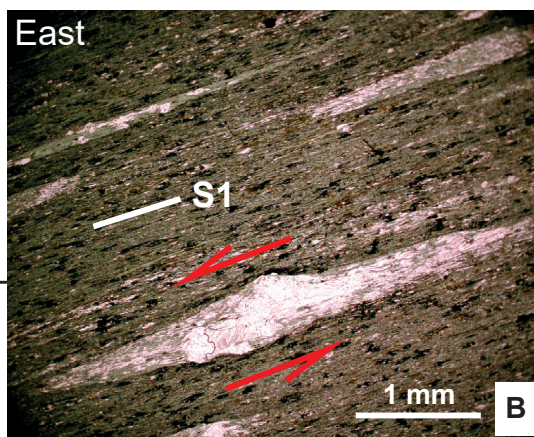
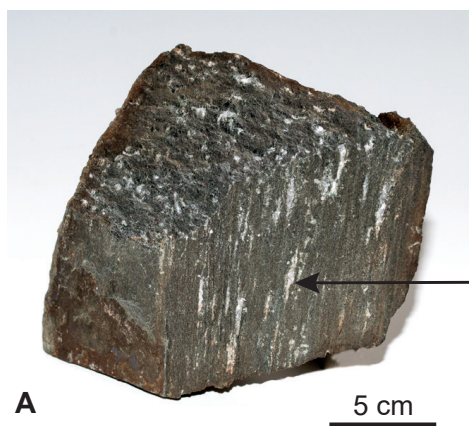


Figure 5. Outcrop photos and interpretations from the Kovo belt. **A.** Kovogruvan (see Fig. 1). A large sulphide-bearing (mainly pyrite) quartz vein along a fault plane juxtaposing metadolerite with strongly-foliated mafic metavolcaniclastic siltstone to the east (not visible in picture). **B.** A strongly-folded phyllitic unit in the upper part of the Kovo group (Harrejaure formation). S-shaped asymmetry indicates tectonic vergence towards the west. **C.** Steeply east-plunging pencil lineations in dolomitic marble (lower Kiruna greenstone group). **D.** Ellipsoidal pillow basalt from the KGG. **E.** Gentle folding of meta-arenites from the Hauki quartzite. **F.** Moderately east-dipping, low-grade shear zone with top-to-the-west sense of shear.

► Figure 6. Microstructures from the Kovo belt. **A.** Rock sample of metavolcanic L>S tectonite from the lower part of the Harrejaure formation (Kovo group). **B.** Microscopic view (crossed polars) from the same sample as in (A). The rods parallel to the mylonitic foliation in the volcanoclastic siltstone indicate eastern-side-down sense of shear (sinistral) and are mainly composed of calcite in the core and quartz in the rims. **C.** East-side-up sense of shear already interpreted from observations on outcrops are confirmed by this asymmetrically-sheared calcite clast. The sample is taken from the upper Kovo group. **D.** Horizontal section from the same outcrop revealing additionally dextral shearing, but with lower strain intensity than the vertical section. **E.** Medium-grade mylonite from the KGG along the contact with the PMS intrusion in the east. Sub-rounded feldspar porphyroclasts recrystallised into polygonal crystalloblastic aggregates. Deviation of the foliation around the porphyroclasts is symmetric and no shear indicators are observed. **F.** Scapolite clast with eye-shaped rim indicates E–W flattening. The sample was taken from a layered basaltic tuff in the upper part of the KGG a few hundred metres from the PMS intrusion. **G.** Folded cleavage in a phyllite from the upper Kovo group indicates E–W shortening with tectonic vergence towards the west. **H.** Fracturing and faulting of lithoclasts (mainly feldspar) surrounded by chlorite indicates shearing parallel to cleavage at relatively low temperatures (>350 °C). The sample was taken from a low-grade shear zone along the eastern contact between the Hauki Quartzite and the KGG.



Geophysical and Geological profiles

Four profiles were constructed to resolve subsurface geometries in the Vakko and Kovo belts (Fig. 7A–D). With a NW–SE orientation, all profiles are oriented roughly orthogonally to the main contacts and structural fabrics. Profile locations were based on the best concentration of available geological and geophysical data. A horizontal projection distance of 200 m of geological data on both sides of the profile was applied, and interpretation depths range between 2 and 3.5 km.

Profile AA'

An additional ground magnetic survey was conducted along the westernmost part of the profile to investigate the nature of the contact between the Archaean basement and the overlying Kovo group (Fig. 7A). Geological evidence for a tectonic contact is derived from moderately foliated and intensively fractured metatonalites, which are locally intersected by metre-wide quartz veins as well as by low-grade, strongly-altered and gold-bearing mylonite zones (see also Luth et al. 2014). Mylonite zones are mostly N–S to N–NE–S–SW-striking and are up to 2 m wide. Mylonitic fabrics consistently indicate an eastern-side-down sense of shear. Based on the interpreted geophysical model, however, a steep eastward-dipping normal shear zone was defined as the main contact between the Archaean basement and the Kovo group. Moreover, within the Kovo group itself, a series of steeply eastward-dipping metadolerites is seen in outcrop as well as in the geophysical modelling results. To the east, a coinciding magnetic and gravity low fits well with the surface expression of the Hauki quartzite. The asym-

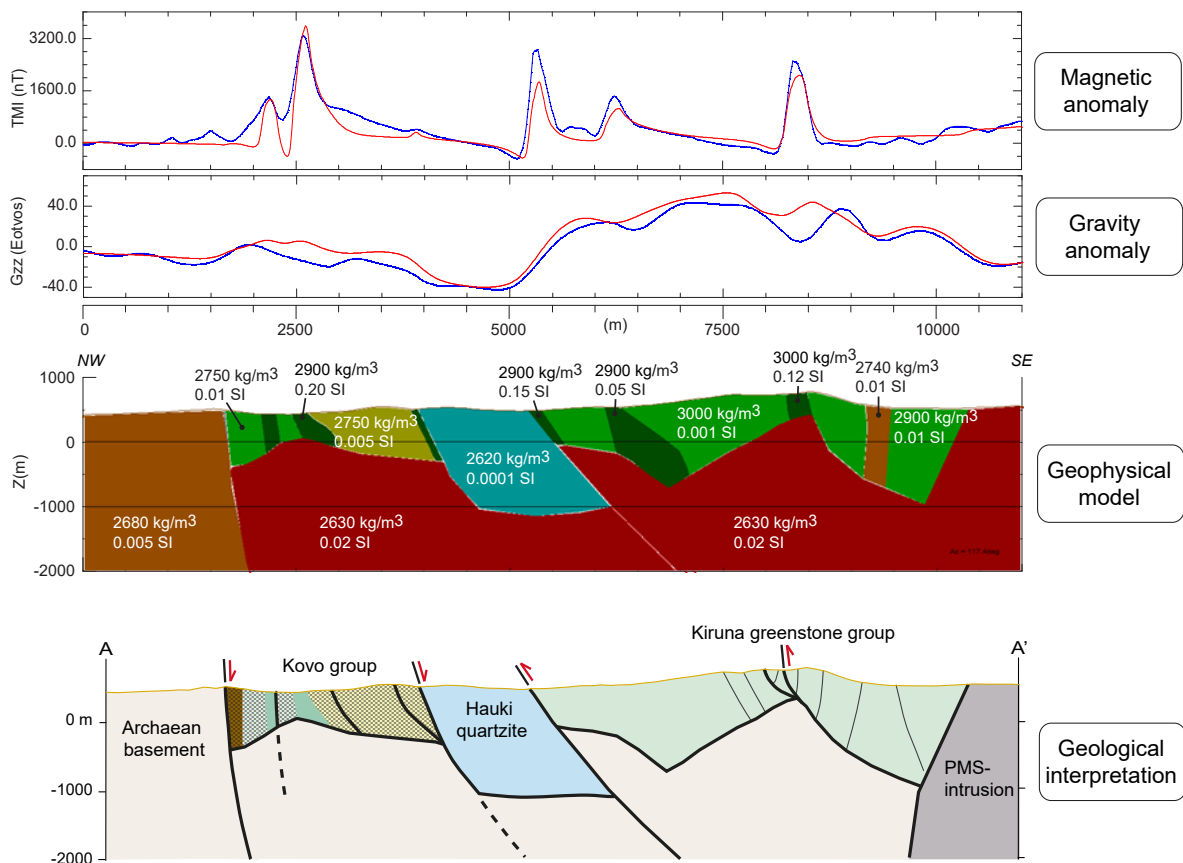


Figure 7A. Profile AA'. The geophysical model is based on airborne magnetic anomalies (upper), gravity (FTG) data (lower) and measured physical rock properties (Table 2). The blue and red graphs plot the measured and calculated values, respectively. Colouring refers to specified physical rock properties highlighted in Table 2. The geological interpretation is based on the geophysical model and geological field observations. Bold lines represent tectonic contacts along shear zones. For colour explanation see the legend in Figure 1.

metric shape of both anomalies indicates that the unit dips to the east and extends to a greater depth (-1100 m) than surrounding units. The western boundary of the Hauki quartzite unit is marked by a shear zone accommodating normal movement as well as a deepening of the underlying basement to the east. In contrast, a relative basement high east of the Hauki quartzite unit should indicate reverse shearing along the contact with the Kiruna greenstone group. Field evidence for both shear zones is lacking due to the absence of exposure along this part of the profile. However, a “look-alike” interpretation of the subsurface outline of the Hauki quartzite unit along profile CC’ does include kinematic field constraints. Further to the east, large depth variations of the Archaean basement underlying the Kiruna greenstone group may be associated with major shear zones and with folding. Large-scale upright folding of the Kiruna greenstone group along profile AA’ near the contact with the PMS intrusion is evident from the pattern seen on magnetic and electromagnetic ground anomaly maps (see also Luth & Antal-Lundin 2013 and Luth et al. 2014).

Profile BB’

The profile intersects the Vakko and Kovo belts and is an extension of a profile published earlier by Martinsson (1999) (Fig. 7B). A large-scale interpretation reveals a moderately southeastward-dipping Archaean basement overlain by supracrustal rock units intersected and bounded by steeply-dipping

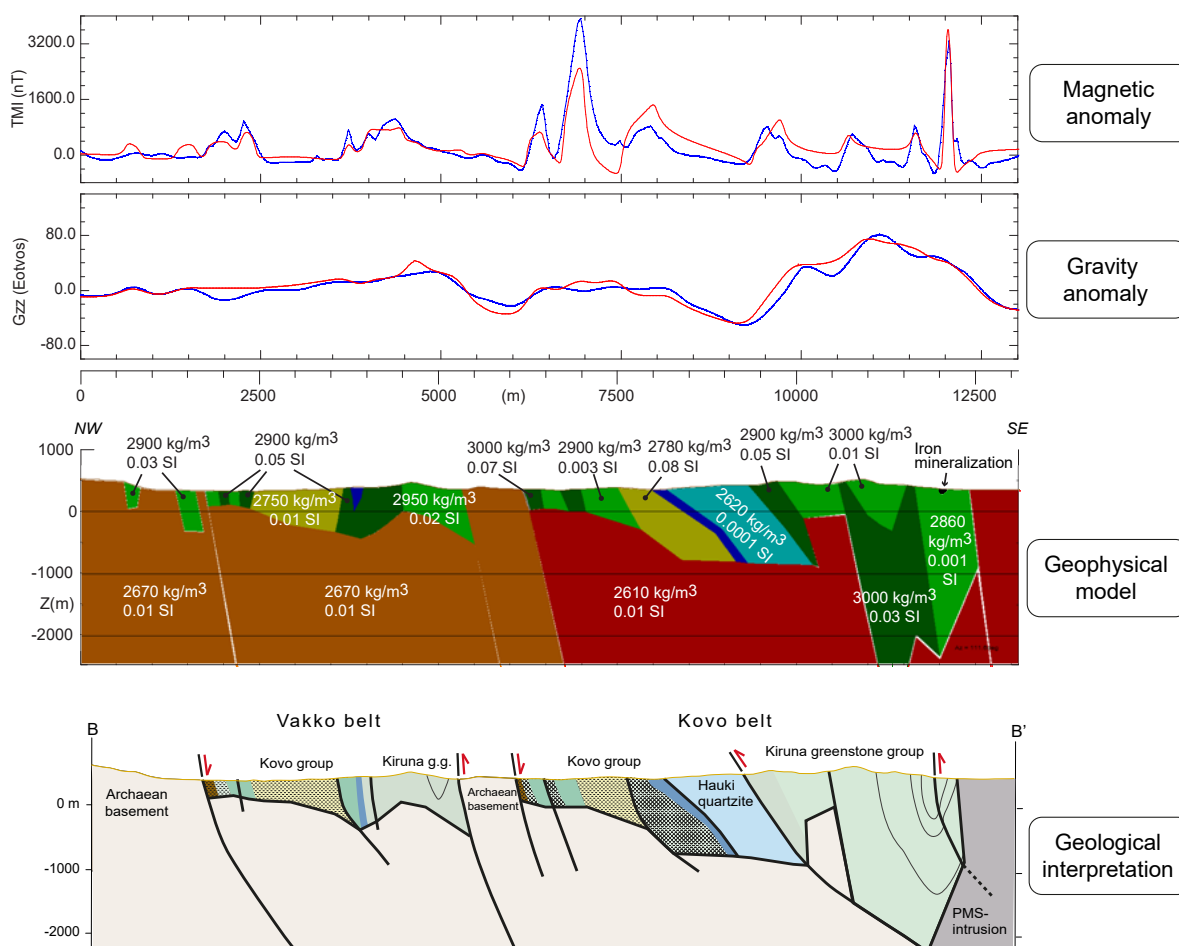


Figure 7B. Profile BB'. The geophysical model is based on airborne magnetic anomalies (upper), gravity (FTG) data (lower) and measured physical rock properties (Table 2). The blue and red graphs plot the measured and calculated values, respectively. Colouring refers to specified physical rock properties highlighted in Table 2. The geological interpretation is based on the geophysical model and geological field observations. Bold lines represent tectonic contacts along shear zones. For colour explanation see the legend in Figure 1.

shear zones. As with profile AA', the tectonic contact between the Archaean basement and the overlying Kovo group dips steeply to the east. A deeper continuation of the shear zone within the Archaean basement is most likely, but evidence is lacking. Field observations along the western border of the Vakko belt indicate tight folding of both the Archaean basement unit and the Kovo group (see also Luth et al. 2014). Foliations and fold axial planes steepen towards vertical in the central and eastern part of the Vakko belt. Underlying local variations in basement depth may be due to folding or faulting. However, a basement high, separating the Vakko and Kovo belts, is bounded by major, steeply southeast-dipping shear zones. As with the Kovo belt, the deepest and easternmost part of the Vakko belt is characterised by a large isoclinal syncline, bounded and possibly intersected to the east by a major shear zone. This shear zone may have accommodated a large amount of east-side-up movement, causing a relative uplift of the Archaean basement, but field constraints on the shear zone's kinematics are lacking. To the east, the part of the profile intersecting the Kovo belt is largely comparable to the corresponding section in profile AA' (Fig. 7A), with the notable exception that the Hauki quartzite unit has a vertical thickness equal to its surrounding units. Normal shearing is localised within the Kovo group to the east of the Hauki quartzite unit, and was inferred from a rapid deepening of the Archaean basement. In contrast, east of the Hauki quartzite, shortening is evident from the tectonic wedge bounding the Kiruna greenstone group. Here, the FTG data show a strong positive anomaly, which can be explained by an abrupt deepening of the basement. In combination with the folding pattern seen on magnetic and slingram anomaly maps, as well as structural field measurements, basement deepening coincides with a large synform, bounded and probably disrupted by the PMS intrusion to the east.

Profile CC'

In comparison with the other profiles, geological interpretations along profile CC' are constrained by a greater number of field observations, and also by several geophysical ground surveys (Fig. 7C). The result portrays a large-scale subsurface structure that has been taken as an example in less well-constrained interpretations of the other profiles. Profile CC' reveals supracrustal units bounded and intersected by major shear zones rooted in the Archaean basement, which deepens to the southeast. The nature of the contact between the Archaean basement and the Kovo group is somewhat ambiguous and appears as a nonconformity where Archaean metatonalites are in contact with conglomerates. Nonetheless, the conglomerates display weak foliation with pebbles that are modestly elongated; no indications of intense shearing were observed. In contrast, intense shearing and a variety of kinematic indicators were observed further to the east of the contact. Here, metavolcanic siltstones directly overlying the basal conglomerates record intense normal shearing in L>S tectonites. 1 to 2 km further east and stratigraphically higher in the Kovo group, reverse shearing in combination with dextral shearing predominates (Fig. 6). Normal shear indicators again become abundant along the contact between the Hauki quartzite and the Kiruna greenstone group. It should be noted in Figure 7C that normal shearing does not accord with subsurface interpretations of the geophysical model, which conversely suggests reverse shearing, causing a vertical offset within the Hauki quartzite. Further east, the Kiruna greenstone group is internally folded along N–S to NE–SW-striking and steeply-dipping axial planes. A slight asymmetry in the folding pattern combined with steeply eastward-dipping shear zones suggests tectonic transportation directed to the northwest. As with profiles AA' and BB', the eastern border of the Kovo belt is characterised by a rapid deepening of the Archaean basement, reaching -2000 m below ground level. The basement is overlain by the Kiruna greenstone group, which is folded into a large syncline. The small gravity increment near the end of the profile is probably due to underlying gabbroic rocks belonging to the PMS intrusion.

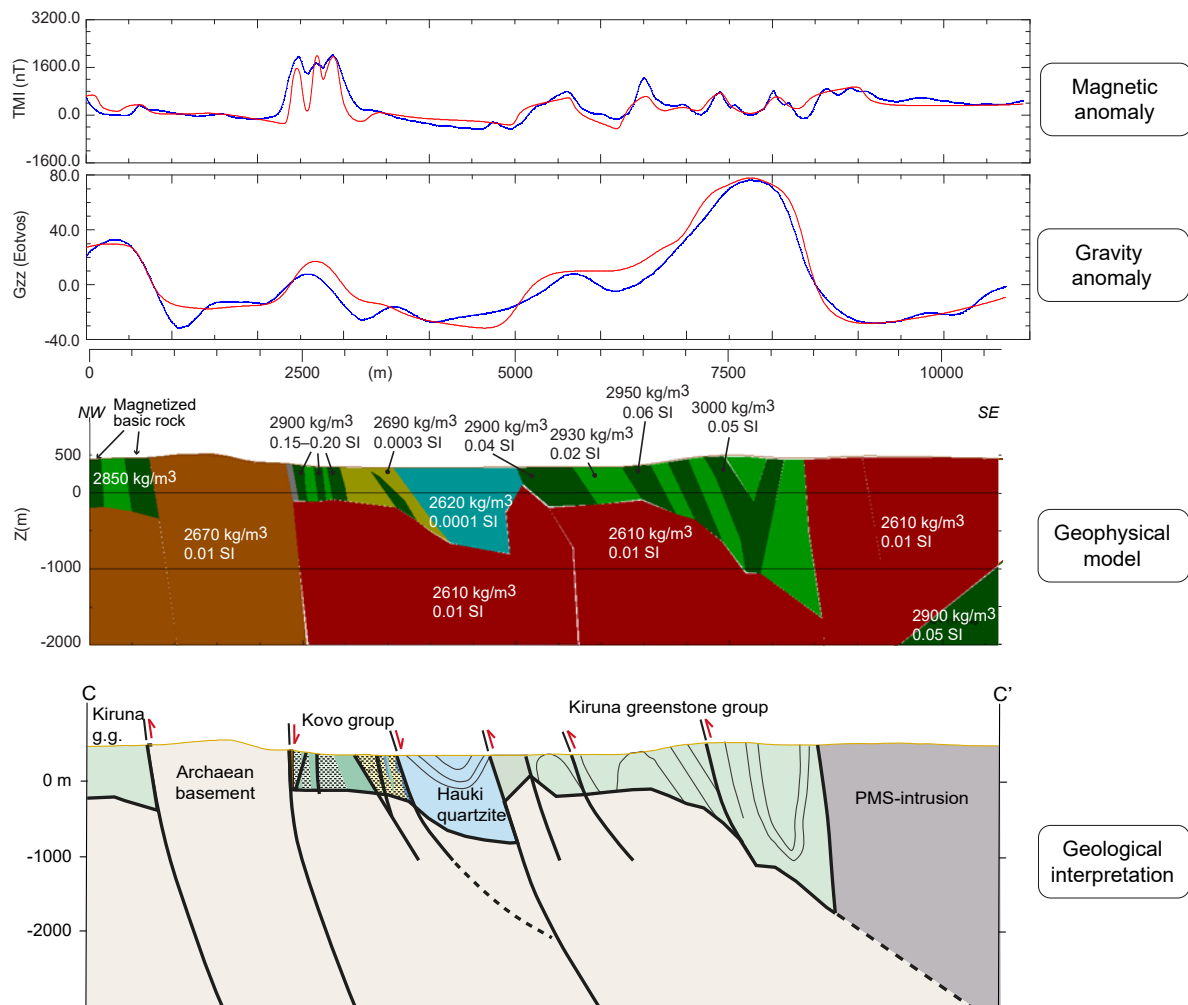


Figure 7C. Profile CC'. The geophysical model is based on airborne magnetic anomalies (upper), gravity (FTG) data (lower) and measured physical rock properties (Table 2). The blue and red graphs plot the measured and calculated values, respectively. Colouring refers to specified physical rock properties highlighted in Table 2. The geological interpretation is based on the geophysical model and geological field observations. Bold lines represent tectonic contacts along shear zones. For colour explanation see the legend in Figure 1.

Profile DD'

Profile DD' is the southernmost profile and aims to connect between subsurface interpretations from the Vakko and Kovo belts and the Kiruna region (Fig. 7D). The profile differs from the northern profiles mainly in the absence of an Archaean basement high separating the Vakko and Kovo belts and the presence of Svecofennian units in place of the PMS intrusion. The resulting geological interpretation highlights the greater depth (3 000 m) of the Archaean basement as the most outstanding feature. A rapid but gradual northwest to southeast deepening of the basement is inferred mainly from the gradually increasing gravity anomaly derived from ground measurements. There are few additional constraints from measured physical properties and geological field data along this part of the profile. Within the Kiruna greenstone group, the magnetic response shows strong variation, allowing interpretations of the subsurface folding pattern. A narrow band of relatively low magnetic anomalies, together with a local gravity low, corresponds to the Hauki quartzite. The unit is wedge-shaped with a maximum depth of only 300 m along its eastern border. East of the Hauki quartzite, the inclusion of northwest-dipping shear zones is primarily based on surface mapping, and the depth extent is uncertain (see Grigull et al., 2018). Further to the east, two narrow magnetic bands surrounding a low

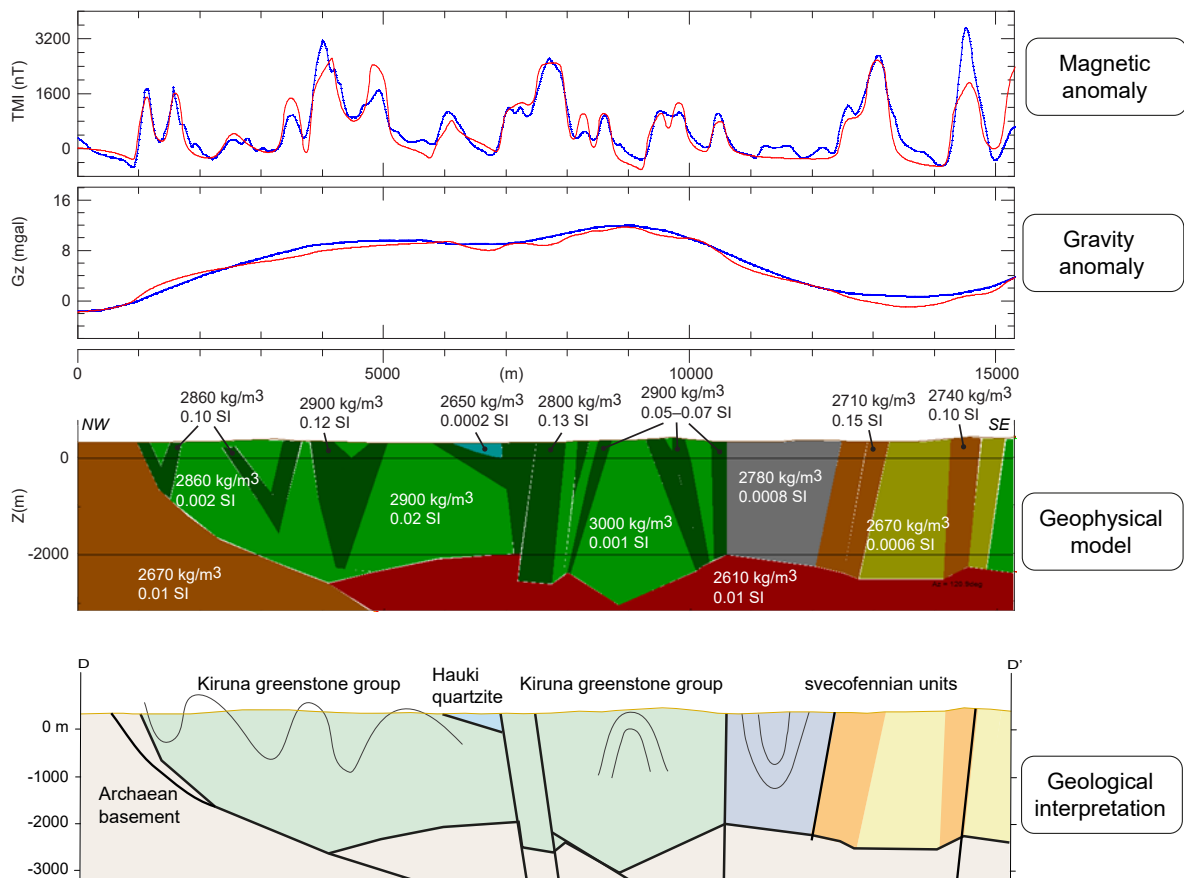


Figure 7D. Profile DD'. The geophysical model is based on airborne magnetic anomalies (upper), gravity (FTG) data (lower) and measured physical rock properties (Table 2). The blue and red graphs plot the measured and calculated values, respectively. Colouring refers to specified physical rock properties highlighted in Table 2. The geological interpretation is based on the geophysical model and geological field observations. Bold lines represent tectonic contacts along shear zones. For colour explanation see the legend in Figure 1.

magnetic core indicate an isoclinal antiform. East of the antiform the Svecofennian units are mainly composed of mica schist and felsic volcanic rocks. Both lithologies have relatively low densities, which is reflected by correspondingly low gravity. The presence of somewhat more dacitic rocks corresponds well with higher magnetic anomalies. Modelling results suggest sub-vertically-oriented units, and is consistent with the steep foliation measured in the field.

DISCUSSION

Tectonic models for the Vakko and Kovo belts

The deformation pattern observed in the Vakko and Kovo belts is most likely the result of a combination of early E–W extension and later NE–SW to E–W-directed shortening. Early extension led to thinning and finally fragmentation of the Archaean basement into separate fault blocks and basins, which then became filled with sediments (see also Kumpulainen 2000). Normal shearing, observed along the major shear zones bounding the Vakko and Kovo belts to the east, may date back to this period of extension. In contrast, and taking into account the 400 Ma time window between the rocks from the Kovo group and the Hauki quartzite, normal shearing observed along the contacts with the Hauki quartzite may be associated with a younger extensional event. Subsequently, crustal shortening inverted the basins and was accommodated by folding, flattening and reverse and dextral shearing

along moderately to steeply southeast-dipping shear zones. The resulting crustal stack mainly comprises supracrustal units, but the Archaean basement was also affected by shortening as it became folded and fragmented.

The PMS intrusion, composed of weakly foliated granite to monzonite and located in the east of the study area, probably formed during or slightly after the main stage of crustal shortening. However, tight, upright folds within the Kiruna greenstone group are warping around the PMS intrusion and may reflect a high amount of shortening in front of a rigid and more competent unit. Likewise, the large syncline marking the eastern border of the Vakko belt may have a comparable origin, where the more competent Archaean basement caused strain localisation. The interpreted tectonic wedge bounded by reverse shear zones within the Kiruna greenstone group in the eastern Kovo belt (profile BB') may also represent crustal "pop-ups" forming directly in front of an indenter in analogue and numerical models (e.g. Davis et al. 1983, Ellis et al. 2004). In the central part of the Kovo belt shortening resulted in predominantly E–W flattening, as well as reverse and dextral shearing. In the northern part of the Kovo belt E–W shortening resulted in local dextral strike-slip along N to NE-striking shear zones. At a later stage the deformed units were intersected by more discrete NW–SE-striking faults accommodating dextral slip as well as vertical, southern-block-up movement.

Deformation resulting from predominantly NE–SW to E–W shortening is largely consistent with the results of earlier geological studies in the Kiruna area (e.g. Wright 1988, Vollmer et al. 1984, Talbot & Koyi 1994). Wright (1988), however, states that all structural features were formed before the intrusion of granite batholiths and that the surrounding supracrustal rocks were not affected by the intrusions. Conversely, Vollmer et al. (1984) concludes that diapirism is a likely explanation for the observed deformation patterns in the area. More recently He et al. (2009) presented an emplacement model for the Fangshan pluton in China, where some structural features are comparable to the PMS intrusion and the eastern part of the Kovo belt, such as a concentric internal pattern of the pluton as well as the presence of an outer rim syncline directly along the contact. However, some other features favouring an emplacement model, such as a high-temperature shear aureole with pluton-side-up kinematic indicators do not accord with our observations.

The depth of the Archaean basement and correlation with the Kiruna area

In the profiles presented, the depth to the Archaean basement varies below the Vakko and Kovo belts from only a few hundred metres in the northwest to more than 2 km in the southeast. A further southward deepening of the Archaean basement is inferred from a comparison between profiles CC' and DD', where the basement reaches a depth of 3 km below the surface (Fig. 8). In line with our observations, recent results from modelling of a seismic reflection survey near Kiruna by Holmgren (2013) and Bastani et al. (2018) have revealed eastward-dipping reflectors originating from lithological boundaries to a depth of approximately 3.5 km. A deepening of the Archaean basement from 2 to 3.5 km over a distance of 6 km probably requires a southward-dipping basement combined with a significant amount of vertical displacement along major shear zones located between the Kovo belt and the Kiruna area. The main candidate along which vertical movements could be accommodated is a series of NW–SE-striking faults interpreted from magnetic anomaly maps northwest of profile DD' (Figs. 1 and 3). Fault zones with a similar orientation crosscutting both the Archaean basement and the overlying Palaeoproterozoic units were mapped earlier throughout the study area, primarily based on geophysical data (e.g. Martinsson 1999), but good geological field observations on those structures are lacking.

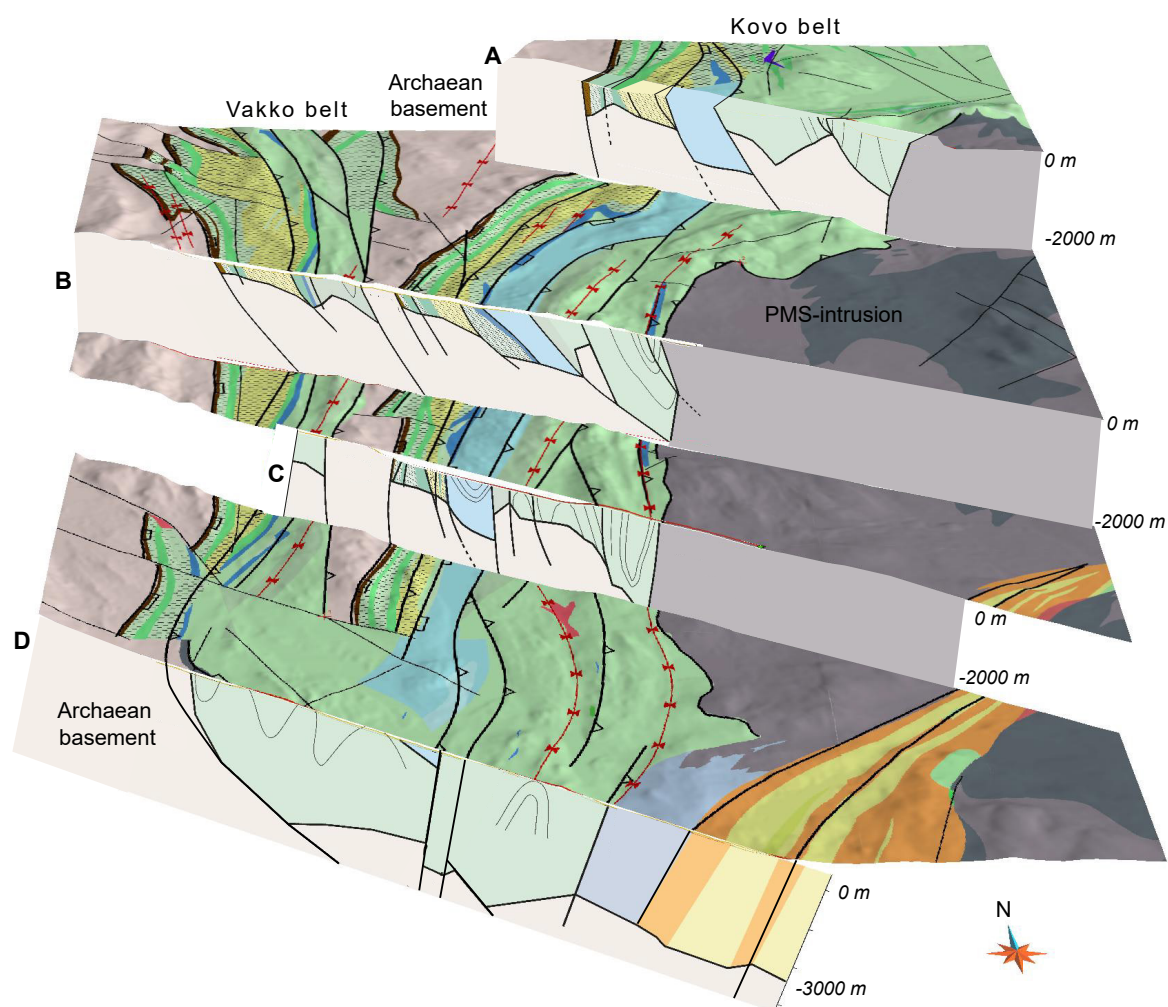


Figure 8. Regional block model for the Vakko and Kovo belts based on a combination of structural geology mapping and geophysical modelling (gravity and magnetic) along 4 transects (Figs. 1 and 3). The area is sliced and translated vertically along each profile to highlight the subsurface structures below the transposed geological map. Map colours are as in Figure 1 and line symbols as in Figure 3.

CONCLUSIONS

Structural geological field investigations combined with geophysical modelling have revealed the 3D structure of the Palaeoproterozoic Vakko–Kovo greenstone belts north of Kiruna. Predominantly steep eastward-dipping shear zones bound and intersect both the Archaean basement and the overlying metasupracrustal units. Shear sense indicators associated with the major shear zones reveal that formation and deformation of the belts occurred during E–W crustal extension, followed by NE–SW to E–W shortening. As such, several major shear zones are thought to have started out as normal shear zones, becoming reactivated and steeped during shortening by reverse shearing or dextral strike-slip. Deformation by shortening also resulted in upright isoclinal folding of both the Archaean basement and the metasupracrustal units. Based on the high amplitude of folds and the recognition of a tectonic wedge, we suggest that some shortening became localised in the eastern parts of the both belts. Localisation of shortening can be attributed to indentation of the adjacent highly competent rocks of the Archaean basement and of the PMS intrusions into the Vakko and Kovo belts, respectively. A 3D correlation between the profiles presented indicates that the shallow to moderately-dipping Archaean basement extends towards the southeast. A rapid southward deepening of the basement from 2 to 3.5 km below Kiruna may be assigned to vertical movements along NW–SE striking fault systems but requires further investigation.

REFERENCES

- Bastani, M., Antal Lundin, I., Savvaidis, A., Kamm, J. & Wang, S., 2015: Barentsprojektet 2014: audio-magnetotelluriska (AMT) mätningar i Kiruna- och Lannavaaraområdet, preliminära resultat. *Sveriges geologiska undersökning SGU-rapport 2015:10*, 16 s.
- Bergman, S., Kübler, L. & Martinsson, O., 2001: Description of regional geological and geophysical maps of northern Norrbotten County. *Sveriges geologiska undersökning Ba 56*, 110 pp.
- Davis, D., Suppe, J. & Dahlen, F. A., 1983: Mechanics of fold-and-thrust belts and accretionary wedges. *Journal of Geophysical Research: Solid Earth*, 88(B2), 1153–1172.
- Ellis, S., Schreurs, G. & Panien, M., 2004: Comparisons between analogue and numerical models of thrust wedge development. *Journal of Structural Geology*, 26(9), 1659–1675.
- Folcker, G., 1974: Urbergsstratigrafisk studie över Vittangivaara, Norrbottens län. *Sveriges geologiska undersökning C 697*, 20 pp.
- Geijer, P., 1927: Vakköjärvdiskordansens stratigrafiska ställning. *Geol. Fören. Förh.* 49, s. 483.
- Geijer, P., 1931: Berggrunden inom malmtrakten Kiruna–Gällivare–Pajala. *Sveriges geologiska undersökning C 366*, 225 pp.
- Godin, L., Parák, T., Espersen, J. & Forsell, P., 1979: Cu i Kirunagrönsten. Slutrapport. LKAB Prospekteringsrapport Ki-04-79, 58 pp.
- Grigull, S., Berggren, R., Jönberger, J., Jönsson, C., Hellström, F.A. & Luth, S., 2018: Folding observed in Palaeoproterozoic supracrustal rocks in northern Sweden. In: Bergman, S. (ed): *Geology of the Northern Norrbotten ore province, northern Sweden. Rapporter och Meddelanden 141*, Sveriges geologiska undersökning. This volume pp 205–257.
- He, B., Xu, Y.-G. & Paterson, S., 2009: Magmatic diapirism of the Fangshan pluton, southwest of Beijing, China. *Journal of Structural Geology* 31: 615–626
- Holmgren J., 2013: Seismic modeling of reflection survey near Kiruna. Bachelor thesis, Luleå University, 41 pp.
- Kumpulainen, R., 2000: The Palaeoproterozoic sedimentary record of northernmost Norrbotten, Sweden. Final report. Stockholm University, Department of geology and geochemistry.
- Kumpulainen, R. A., 2003: Svecofennian sedimentary record of northern Sweden. Unpublished report, Sveriges geologiska undersökning, 20 pp.
- Luth, S. & Antal-Lundin, I., 2013: Summary report on the geological and geophysical characteristics of the Harijärvet-Vittangivaara key areas. *Sveriges geologiska undersökning Report SI313*.
- Luth, S., Lynch, E.P., Grigull S., Thörnelöf, M., Berggren, R. & Jönberger, J., 2014: Geological and geophysical studies in the Harijärvet, Vittangivaara and Akkiskera-Kuormakka key areas. *Sveriges geologiska undersökning SGU-rapport 2014:09*, 24 s.
- Martinsson O., 1997: Paleoproterozoic greenstones at Kiruna in northern Sweden: a product of continental rifting and associated mafic-ultramafic volcanism. In: O. Martinsson: *Tectonic setting and metallogeny of the Kiruna greenstones. Doctoral thesis 1997:19, Paper I*, 1–49. Luleå University of technology.
- Martinsson, O., 1999: Bedrock map 30J Rensjön NO, scale 1:50 000. *Sveriges geologiska undersökning Ai 131*.
- Martinsson, O., Vaasjoki, M. & Persson, P.-O., 1999: U-Pb ages of Archean to Palaeoproterozoic granitoids in the Torneträsk-Råstojäure area, northern Sweden. In: S. Bergman (ed.): *Radiometric dating results 4. Sveriges geologiska undersökning C 831*, 70–90.
- Ödman, O.H., 1957: Beskrivning till berggrundskarta över urberget i Norrbottens län. *Sveriges geologiska undersökning Ca 41*, 151 pp.
- Offerberg, J., 1967: Beskrivning till Berggrundskartbladen Kiruna NV, NO, SV, SO. *Sveriges geologiska undersökning Af1–4*, 147 pp.
- Skiöld, T., 1979: Zircon ages from an Archean gneiss province in northern Sweden. *Geologiska Föreningens i Stockholm Förhandlingar* 103, 169–171.
- Skiöld, T., 1986: On the age of the Kiruna Greenstones, northern Sweden. *Precambrian Research* 32, 35–44.
- Talbot, C.J. & Koyi, H., 1995: Paleoproterozoic intraplating exposed by resultant gravity overturn near Kiruna, northern Sweden. *Precambrian Research* 72, 199–225.
- Vollmer, F.W., Wright, S.F. & Huddleston, P.J., 1984: Early deformation in the Svecokarelian greenstone belt of the Kiruna district, northern Sweden. *Geologiska Föreningens i Stockholm Förhandlingar* 106, 109–118.
- Welin, E., Christiansson, K. & Nilsson, Ö., 1971: Rb-Sr radiometric ages of extrusive and intrusive rocks in Northern Sweden. *Sveriges geologiska undersökning C 666 I-38* 40.
- Witschard, F., 1984: The geological and tectonic evolution of the Precambrian of northern Sweden – a case for basement reactivation? *Precambrian Research* 23, 273–315.
- Wright, S.F., 1988: Early Proterozoic deformational history of the Kiruna district, northern Sweden. Unpublished Ph.D. thesis. University of Minnesota, 170 pp.



Geological Survey of Sweden
Box 670
SE-751 28 Uppsala
Phone: +46 18 17 90 00
Fax: +46 18 17 92 10
www.sgu.se

Uppsala 2018
ISSN 0349-2176
ISBN 978-91-7403-393-9
Tryck: Elanders Sverige AB